Chapter 8
In vitro cell line studies

8.1 Introduction

After optimization and characterization, the final objective was to deliver the drug loaded NPs by parenteral route but before administration formulations has to be evaluated for their safety and efficacy in cancerous cell lines. Performance of non-targeted and targeted NPs was evaluated by the cell uptake, cell cytotoxicity/cell viability, cell cycle analysis and apoptosis studies in breast cancer cell lines.

8.2 Materials

Rhodamine B and 6-Coumarin dye were purchased from Sigma-Aldrich, Mumbai, India. Leibovitz L-15 medium, Minimum essential medium (MEM), Fetal bovine serum (FBS), Antibiotic antimycotic solution and Trypsin-EDTA were purchased from Himedia Lab. Pvt. Ltd., Mumbai, India. Sodium chloride (NaCl), Potassium chloride (KCl), Sodium hydrogen phosphate dihydrate ($Na_2HPO_4 \cdot 2H_2O$) and Potassium dihydrogen phosphate (KH_2PO_4) were purchased from H. B. Chemical, Vadodara, India. Triton X-100, Sodium deoxycholate, Sodium dodecyl sulphate (SDS), Tris Hydrochloride, EDTA and Protease inhibitor cocktail were purchased from Sigma Aldrich, USA. 6-well plates, 96-well plates, tissue culture flask (25 and 75 cm^2), chamber slide and other sterile material for cell culture were purchased from Thermo scientific, India. Annexin V-FITC apoptosis detection kit was obtained from BD Pharmingen, CA, USA. 4,6-diamidino-2-phenylindole (DAPI) was purchased from Invitrogen, Mumbai, India. All other chemicals were of analytical reagent grade and obtained commercially.

8.2.1 Primary and Secondary Antibodies

Anti-EGFR mouse monoclonal antibody was purchased from Santa Cruz Biotechnology, USA. Secondary antibody (Horseradish peroxidase (HRP)-conjugated goat anti-mouse IgG and FITC-conjugated goat anti-mouse IgG) were purchased from Beijing Huamei Biotechnology (Beijing, China).

8.2.2 Cell lines

MDA-MB-468 and MCF-7 cell line were purchased from NCCS, Pune, India. MDA-MB-231 cell line was obtained from Indian Institute of Chemical Technology, Hyderabad, India. EGFR positive (MDA-MB-468 and MDA-MB-231) cell lines were cultured in Leibovitz L-15 medium and EGFR negative (MCF-7) cell line was cultured

MEM medium. All cell lines medium were supplemented with 10% (v/v) FBS and 1% antibiotic antimycotic solution (containing Penicillin G, Streptomycin and Amphotericin B) and incubated at 37 °C in a 5% CO_2 incubator.

8.2.3 Equipments

- SDS-PAGE electrophoresis chamber (Genaxy Scientific Pvt. Ltd., USA)
- GelDoc™ XR^+ Imaging System (BioRad, USA)
- ELISA plate reader (Bio-Rad, USA)
- Confocal laser scanning microscope, LSM 710 (Carl-Zeiss Inc., USA)
- Jouan IGO150 5% CO_2 incubator (Thermo-Fischer, Germany)
- Weiber vertical Laminar Air Flow (Weiber, India)
- Nikon H600L Microscope (Nikon, Japan)
- Fluorescence activated cell sorter (FACS- BD-AriaIII, USA)

8.3 Methods

8.3.1 Receptor expression (EGFR) analysis by Western Blot

Western blotting or immunoblotting is a method used for identifying a specific protein in a complex mixture along with determination of its molecular weight. Heating of cell lysates with sample buffer containing SDS, an anionic surfactant, and dithiothreitol (DTT) (or Tris(2-carboxyethyl) phosphine, TCEP) as reducing agent, reduces protein disulphide bonds to thiol groups and disrupt non-covalent bonds in the proteins, denaturing them, and causing the molecules to lose their native conformation. Protein samples are first electrophoresed on SDS-PAGE and in this process proteins migrate through the gel and separated according to their size and charge. These separated proteins are electrotransferred onto nitrocellulose/PVDF membrane for further analysis. To detect the protein (antigen) blotted on the membrane, it is incubated with an antibody (primary) specific for the protein of interest. The membrane is then incubated with a second antibody (secondary) which is specific for the primary antibody. The secondary antibodies are covalently attached to an enzyme, e.g. alkaline phosphatase or horseradish peroxidase. These enzymes form a coloured precipitate upon reacting with a chromogenic substrate. As a result a visible band can be seen on the membrane where the primary antibody is bound to the protein (1).

Protocol:

1. 3 $\times 10^5$ cells of different cell lines (MCF-7, MDA-MB-468 and MDA-MB-231) were seeded in culture flask (75 cm^2) and allowed to reach 90 % confluency. Thereafter, the cells were trypsined and collected by centrifugation.
2. The cells were lysed in RIPA buffer (Radio Immuno Precipitation Assay buffer) (150 mM NaCl, 0.1% Triton X-100, 0.5 % sodium deoxycholate, 0.1% SDS, 50 mM Tris-HCL pH 8.0, 2 mM EDTA) containing 1% protease inhibitor cocktail and incubated for 30 min. Subsequently, the lysates were centrifuged (12,000 rpm for 15 min at 4 °C) and the supernatants were used for further analysis.
3. Protein concentration was determined by BCA method.
4. Aliquots of each sample containing 50 µg proteins were resolved on a SDS-polyacrylamide gel, by electrophoresis at 30 mA for 2 h.
5. PVDF membrane was cut according to the size of the gel. The resolved gel and the membrane both were equilibrated with the transfer buffer for 15 minutes.
6. After equilibration the membrane was kept over the gel and this was sandwiched between the folds of filter paper, two on either side. Care was taken to avoid any bubbles to be trapped.
7. The sandwich was then kept between the electrode plates of the transfer assembly. The transfer assembly was filled with the transfer buffer. Transfer was carried out for 14 hr at constant 10 V or for 1 hr at 100 V in a cold room.
8. Membranes were then probed with primary antibody specific to EGFR diluted at 1:2000 v/v. The membranes were washed three times with PBS containing 1% Tween 80 and probed with goat anti-mouse secondary antibody diluted at 1:250 v/v.
9. Protein bands were detected using chemiluminescence and densitometric analysis was carried out using quantity one Quantitation software.

8.3.2 MTT assay/ Cell Cytotoxicity

It is a colorimetric assay that measures the reduction of yellow 3-(4,5-dimethythiazol-2-yl)-2,5-diphenyl tetrazolium bromide (MTT) by mitochondrial succinate dehydrogenase. MTT enters the cells and passes into the mitochondria where it is reduced by mitochondrial dehydrogenases in living cells to a blue-magenta coloured formazan crystals. The absorption of dissolved formazan in the visible region correlates with the number of intact alive cells, since the reduction of MTT can only

occur in metabolically active cells the level of activity estimates number of viable cells. Tetrazolium dye reduction is dependent on NAD(P)H dependent oxidoreductase enzymes largely in the cytosolic compartment of the cell. Therefore, reduction of MTT and other tetrazolium dyes increases with cellular metabolic activity due to elevated NAD(P)H flux. Cytotoxic compounds are able to damage and destroy cells, and thus decrease the reduction of MTT to formazan (2, 3).

Protocol:

1. MCF-7/MDA-MB-468/MDA-MB-231 cells were seeded in 96-well plate ($5x10^3$ cells/well) and allowed to attach and grow.
2. After 24 h, the medium was removed and treated different formulations of different concentration and incubated for different time periods.
3. After incubation, treatment media was removed and cells were treated with 20 µl (5 mg/ml) of MTT dye [3-(4,5-dimethylthiazoyl-2-yl)-2,5-diphenyl tetrazolium bromide] and incubated for 2 hrs.
4. The medium from each well was discarded and resulting formazan crystals were solubilized in 200 µl of dimethylsulphoxide and quantified by measuring absorbance at 570 nm using an enzyme-linked immunosorbent assay (ELISA) plate reader.

8.3.3 Cellular uptake

The mechanism of cellular internalization of macromolecules is the primary advantage as drug delivery vehicles. Cells possess a variety of active internalization mechanisms to accommodate cellular entry of large molecular complexes because cell membrane is naturally impermeable to complexes larger than 1 kDa. Endocytosis is a process through which the cell membrane will invaginate to engulf molecules and extracellular fluid in an intracellular membrane bound vesicle or endosome, which will subsequently travel through the cell (4). To enable their retention; NPs may reside near the membrane or directly interact with membrane proteins. Analogous to the attachment of drug moieties to high molecular weight carriers, agents such as antibodies, antibody fragments, scFv and other high affinity ligands can be conjugated on the surface of NPs in order to exploit direct membrane interactions and target the delivery system to specific cell populations in organ systems. Not only the cellular recognition of these carriers but also the trafficking pathway and subcellular localization within the cell is regulated by targeting macromolecular complexes with

high affinity ligands specific to membrane proteins, namely receptors (5). The major objective for targeted drug delivery is to reduce the non-selective uptake of toxic agents and to enhance drug accumulation at the target site. In order to target the drug delivery system to specific organ/tissue system within the body, targeting agent can be directly attached to drug molecules or complexed with a vehicle (6). Cell uptake studies were carried out using 6-Coumarin (lipophilic fluorescent dye for DTX) and Rhodamine B (hydrophilic fluorescent dye for VBT) loaded NPs with the aim of finding whether the NPs are internalized into the cells and to determine the intracellular concentrations of the loaded dye.

8.3.3.1 Confocal microscopy

Confocal laser scanning microscopy (CLSM) is a technique for obtaining high-resolution optical images. The most common applications of confocal microscopy are the analysis of mechanisms of cell functioning and disease mechanisms. The ability to stain organelles and proteins allows detailed mechanistic studies to be performed on live cells in a time-resolved manner. Sub-cellular localisation of nanoparticles can be tracked in a time-resolved manner, with co-staining of organelles (7, 8).

Protocol for qualitative cellular uptake by confocal microscopy:

1. 1×10^4 MCF7/MDA-MB-468/MDA-MB-231 cells were seeded onto 6-well plates with a glass cover slip at the bottom and allowed to attach and grow for 24 hr.
2. After 24 hr the cells were incubated with 100 µl, 10 µg/ml 6-Coumarin, 6-Coumarin loaded HSA NPs and 6-Coumarin loaded INPs for 6 h as well as cells were incubated with 100 µl, 10 µg/ml Rhodamine, Rhodamine loaded HSA NPs and Rhodamine loaded INPs.
3. After 6 hrs treatment the formulations were removed and adhered cells were washed 3 times with 1× PBS.
4. 100 µl ice cooled 4 % paraformaldehyde (PFA) was added and kept for 10 min for fixing.
5. After 10 min PFA was removed and washed 3 times with 1× PBS and treated with 100 µl (1 µg/ml) DAPI for 15 min.
6. After 15 min DAPI was removed and cells washed again 3 times with 1× PBS.
7. Cover slips were mounted on slides after washing with PBS three times using glycerol as mounting agent and the resulting slides were visualized under confocal laser scanning microscope. (LSM 710, Carl-Zeiss Inc., USA).

8.3.3.2 Fluorescence-activated cell sorting (FACS)

FACS is a specialized type of flow cytometry. It provides a method for sorting a heterogeneous mixture of biological cells into two or more containers, one cell at a time, based upon the specific light scattering and fluorescent characteristics of each cell. It is a useful scientific instrument, as it provides fast, objective and quantitative recording of fluorescent signals from individual cells as well as physical separation of cells of particular interest (9).

The cell suspension is entrained in the centre of a narrow, rapidly flowing stream of liquid. The flow is arranged so that there is a large separation between cells relative to their diameter. A vibrating mechanism causes the stream of cells to break into individual droplets. The system is adjusted so that there is a low probability of more than one cell per droplet. Just before the stream breaks into droplets, the flow passes through a fluorescence measuring station where the fluorescent character of interest of each cell is measured. An electrical charging ring is placed just at the point where the stream breaks into droplets. A charge is placed on the ring based on the immediately prior fluorescence intensity measurement, and the opposite charge is trapped on the droplet as it breaks from the stream. The charged droplets then fall through an electrostatic deflection system that diverts droplets into containers based upon their charge. In some systems, the charge is applied directly to the stream, and the droplet breaking off retains charge of the same sign as the stream. The stream is then returned to neutral after the droplet breaks off.

Protocol for quantitative cellular uptake by FACS:

1. 1×10^5 MCF7/MDA-MB-468/MDA-MB-231 cells were seeded on 6-well plate and allowed to attach and grow for 48 h.
2. After 48 h of proliferation, cells were treated with 1 ml medium containing different formulations (For hydrophobic drug (DTX): 6-Coumarin, 6- Coumarin HSA NPs and 6-Coumarin HSA INPs) and (For hydrophilic drug (VBT): Rhodamine, Rhodamine HSA NPs and Rhodamine HSA INPs) at a concentration of 100 µg/ml for 60, 120 and 180 min.
3. After incubation, the cells were harvested and washed three times with cold PBS having pH = 7.4 and then analyzed by FACS for total amount of NPs uptake by 10,000 cells.

8.3.4 Apoptosis

A process of Programmed cell death that may occur in multicellular organisms is called as apoptosis. Biochemical events lead to characteristic cell changes and death. Changes in morphological and biochemical characteristic shown by the cells undergoing apoptosis include chromatin aggregation, nuclear and cytoplasmic condensation, while necrosis displays a direct injury to the cell. To compare the effectiveness of NPs formulations the determination of cell death mechanism is very important. Apoptosis study of prepared NPs was conducted using Annexin V staining procedure. This assay takes advantage of the fact that phosphatidylserine (PS) is translocated from the inner (cytoplasmic) leaflet of the plasma membrane to the outer (cell surface) leaflet soon after the induction of apoptosis. Annexin V is a 35-36 kDa Ca^{2+} dependent phospholipid-binding protein that has a high affinity for PS, and binds to cells with exposed PS. Annexin V may be conjugated to fluorochromes including FITC. This format retains its high affinity for PS and thus serves as a sensitive probe for flow cytometric analysis of cells that are undergoing apoptosis (10, 11).

Protocol:

1. 1×10^5 MDA-MB-468/ MDA-MB-231 cells were seeded on 6-well plates and allowed to attach and grow for 24 h.
2. Cells were treated with 2 ml media containing 1 µg/ml Taxotere, DTX-HSA-NPs, DTX-HSA-INPs and incubated for 24 and 48 h whereas cells treated with 2 ml media containing 1 µg/ml Navelbine, VBT-HSA-NPs and VBT-HSA-INPs incubated for 48 and 60 h.
3. After incubation, cells were harvested and centrifuged at 2,000 rpm for 5 min.
4. Cells were suspended in 100 µl binding buffer and stained with Annexin V-FITC (2 µl) and incubated for 15 min at room temperature with light protection.
5. After incubation, Propidium Iodide (PI) (2 µl, 50 µg/ml) was added and incubated at 4 °C for 10-15 min. After incubation, 200 µl of additional binding buffer was added, and suspension was analysed using FACS.
6. The intensity plot was sectioned in four quarters to differentiate stained and unstained cells. Based on four quarters, percentage of cells in early apoptotic phase (FITC positive and PI negative), late apoptotic phase (FITC and PI positive), necrotic phase (FITC negative and PI positive) and viable cells (FITC and PI negative) were recorded.

8.3.5 Cell cycle analysis

Cellular growth is considered as successive phases, characterized by specific biochemical processes and called as cell cycle. Flow cytometry was used to determine the distribution of DNA in the cell replication state (12). Quiescent and G1 cells will have one copy of DNA having 1X fluorescence intensity. G2/M phase of the cell cycle will have two copies of DNA having 2X fluorescence intensity. S phase synthesizing DNA they will have fluorescence values between the 1X and 2X populations.

Protocol:

1. MDA-MB-468/ MDA-MB-231 cells were seeded onto 6-well plates at a density of 1 x 10^6 cells/well and allowed to attach and grow for 24 h.
2. After 24 h of seeding cells were treated with 2 ml media containing 1 µg/ml Taxotere, DTX-HSA-NPs, DTX-HSA-INPs for 24 h and Navelbine, VBT-HSA-NPs and VBT-HSA-INPs for 60 h.
3. After incubation, medium was removed in to individual tubes. Cells were washed with 1× PBS and harvested with 200 µl of trypsin-EDTA.
4. Cells were collected and centrifuged at 2000 rpm for 5 min. The cell pellet was washed twice with PBS and centrifuged.
5. Cells were re-suspended in 2 ml ethanol (70%) for fixing and kept at -20 °C for 30 min. Cells were centrifuged and were lysed in 250 µl 1× PBS containing 0.2% triton X 100 and incubated at 4 °C for 30 min.
6. They were again centrifuged and re-suspended in 500 µl 1× PBS containing 20 µl RNAse (10 mg/ml) and incubated at 37 °C for 30 min. Cells were then centrifuged and re-suspended in 500 µl of 1× PBS containing 10 µl PI (1 mg/ml) and incubated for 10-15 min at 4 °C.
7. Samples were transferred to the flow cytometer and cell fluorescence was measured. Maximum excitation of PI bound to DNA was at 536 nm, and emission was at 617 nm. Blue (488 nm) or green light lines of lasers were optimal for excitation of PI fluorescence on FACS.
8. Histogram of count vs. intensity was made to calculate ratio of cells under G0/G1 (2n), S (2n+), G2/M phase (4n) and under apoptosis (2n-).

8.4 Results and Discussion

8.4.1 Receptor expression (EGFR) in cell lines

The drug INPs were prepared with the objective of receptor mediated endocytosis in EGFR positive breast tumor cells for preferential accumulation of drug at tumor site. To achieve this, expression levels of EGFR in breast cancer cell lines MDA-MB-468 (EGFR Positive), MDA-MB-231 (EGFR Positive) and MCF-7 (EGFR Negative) were assessed by western blotting. The results confirmed the expression of EGFR in MDA-MB-468 and MDA-MB-231 cell line and absence of this receptor in MCF-7 cell line as shown in **Figure 8.1.** EGFR having molecular weight 170 kDa and in western blotting analysis band was observed near 170 kDa (Between 140 to 200 kDa) compared to protein marker in MDA-MB-468 and MDA-MB-231 cell lines and absence of this band in MCF-7 cell line. Thus, MDA-MB-468 and MDA-MB-231 cell line used as positive and MCF-7 cell line used as negative control in further studies respectively.

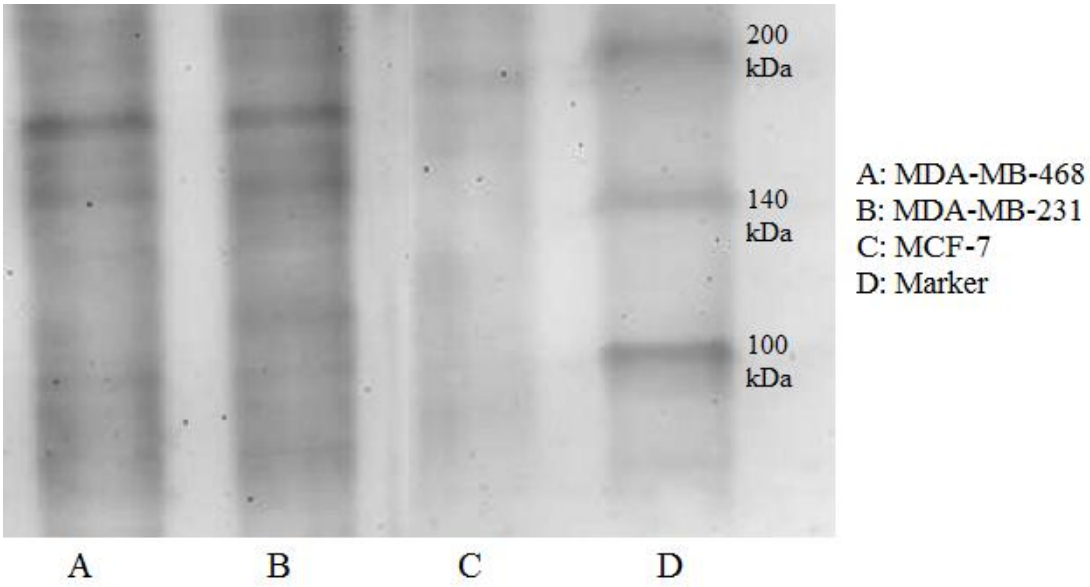

Figure 8. 1 Receptor expression analysis in cell lines.

8.4.2 *In vitro* cytotoxicity studies (MTT assay)

MTT assay is a widespread method to assess cell cytotoxicity. *In vitro* cytotoxicity studies were performed on EGFR positive (MDA-MB-468 and MDA-MB-231) and EGFR negative (MCF-7) cell line and it is demonstrated that scFv EGFR antibody conjugated NPs showed higher cytotoxicity compared to non targeted NPs at

all concentrations and at all-time points in MDA-MB-468 and MDA-MB-231 cells than MCF-7 Cells. % Cell viability and IC_{50} value were determined for Taxotere, DTX-HSA-NPs and DTX-HSA-INPs in MCF-7, MDA-MB-468 and MDA-MB-231 breast cancer cell lines and data presented in **Table 8.1** and **Table 8.2.** Enhanced cytotoxic activity of DTX-HSA-INPs for MDA-MB-468 and MDA-MB-231 cells compared to MCF-7 cells clearly demonstrates the high affinity of INPs towards EGFR positive cancer cells.

Table 8. 1 % Cell viability values of Taxotere, DTX-HSA-NPs and DTX-HSA-INPs in MCF-7, MDA-MB-468 and MDA-MB-231 breast cancer cell lines.

Formulation Concentration (15 µM/ ml)	% Cell viability* (After 6 h)			% Cell viability* (After 24 h)		
	MCF-7	MDA-MB-468	MDA-MB-231	MCF-7	MDA-MB-468	MDA-MB-231
Taxotere	67.21 ± 0.11	68.65 ± 0.42	72.51 ± 0.53	25.31 ± 0.12	28.24 ± 0.35	33.21 ± 0.42
DTX-HSA-NPs	33.15 ± 0.95	39.28 ± 0.63	37.43 ± 0.82	11.39 ± 0.97	15.21 ± 0.68	13.39 ± 0.63
DTX-HSA-INPs	38.25 ± 0.76	18.24 ± 0.89	22.18 ± 0.65	14.51 ± 0.57	8.31 ± 0.78	10.63 ± 0.74

* The experiment was performed in triplicate (n=3)

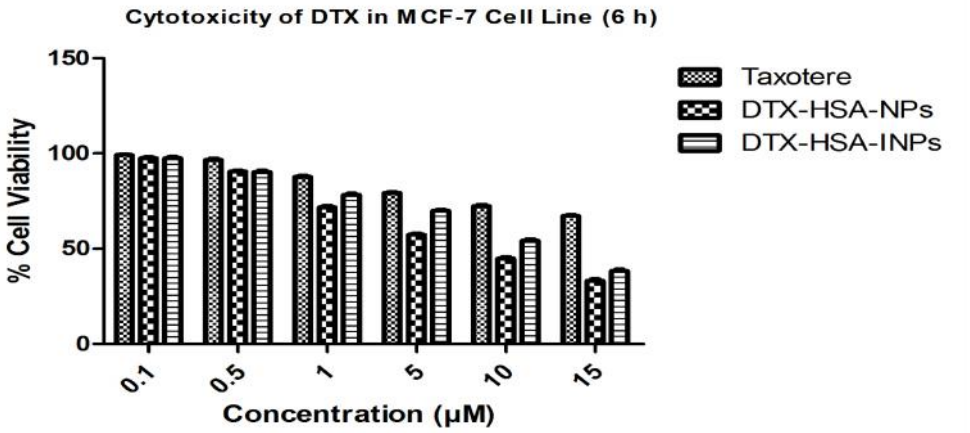

Figure 8. 2 Cytotoxicity of Different Formulations of DTX in MCF-7 Cell-line.

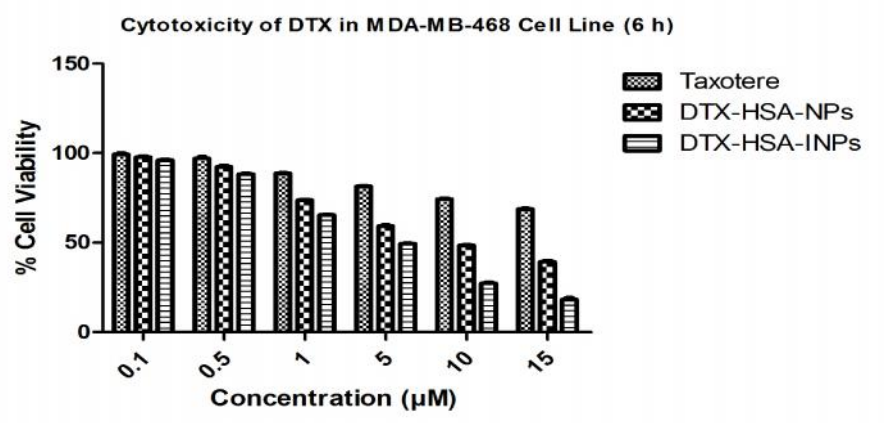

Figure 8. 3 Cytotoxicity of Different Formulations of DTX in MDA-MB-468 Cell-line.

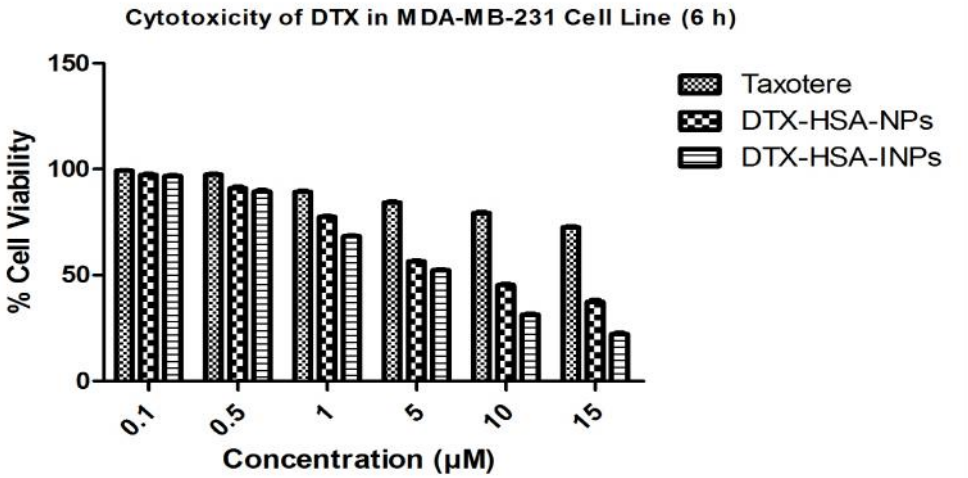

Figure 8. 4 Cytotoxicity of Different Formulations of DTX in MDA-MB-231 Cell-line.

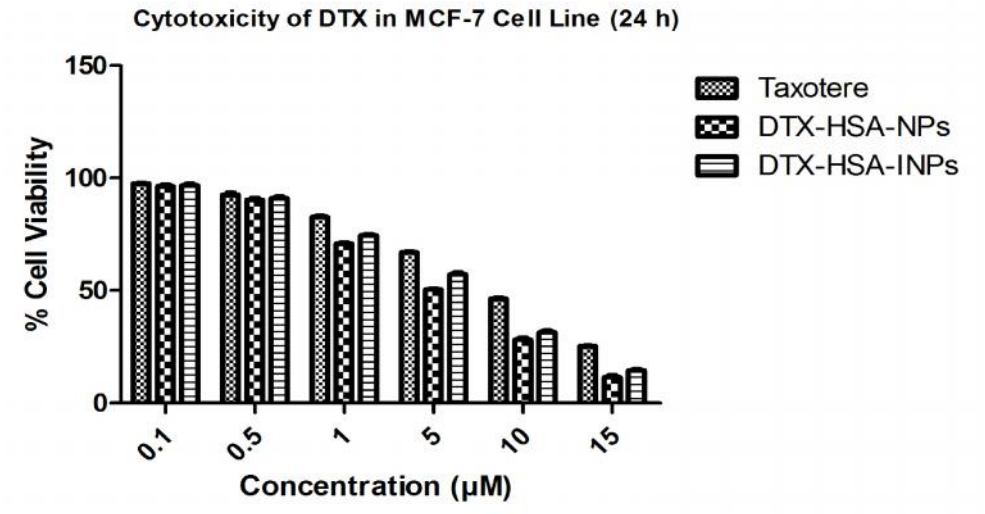

Figure 8. 5 Cytotoxicity of Different Formulations of DTX in MCF-7 Cell-line.

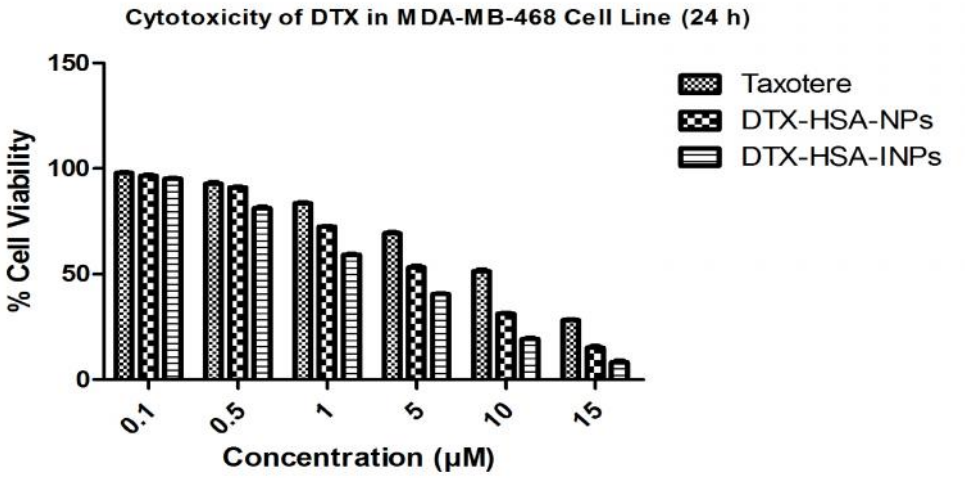

Figure 8. 6 Cytotoxicity of Different Formulations of DTX in MDA-MB-468 Cell-line.

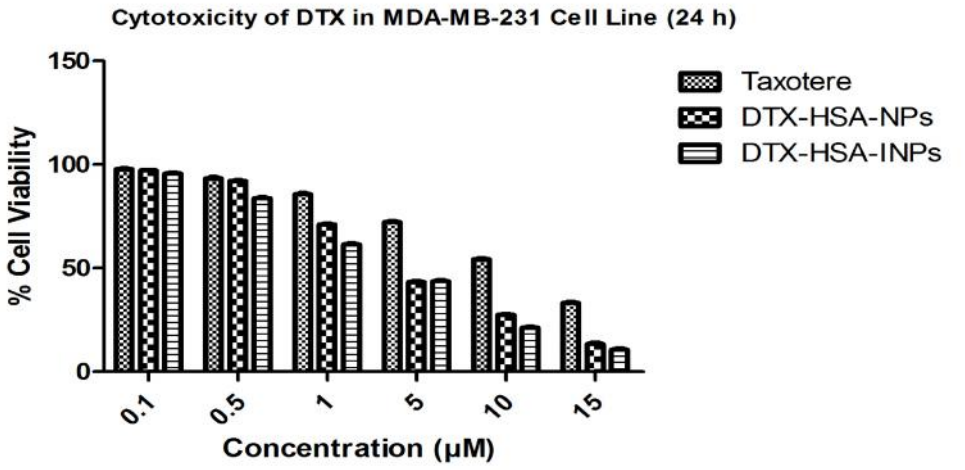

Figure 8. 7 Cytotoxicity of Different Formulations of DTX in MDA-MB-231 Cell-line.

Table 8. 2 IC_{50} Value values of Taxotere, DTX-HSA-NPs and DTX-HSA-INPs in MCF-7, MDA-MB-468 and MDA-MB-231 breast cancer cell lines.

Formulation	IC_{50} Value (µM) (After 6 h)			IC_{50} Value (µM) (After 24 h)		
	MCF-7	MDA-MB-468	MDA-MB-231	MCF-7	MDA-MB-468	MDA-MB-231
Taxotere	26.760	29.666	38.044	8.078	9.979	11.229
DTX-HSA-NPs	7.243	8.921	7.790	3.725	4.330	3.544
DTX-HSA-INPs	10.732	3.773	4.572	4.362	2.050	2.459

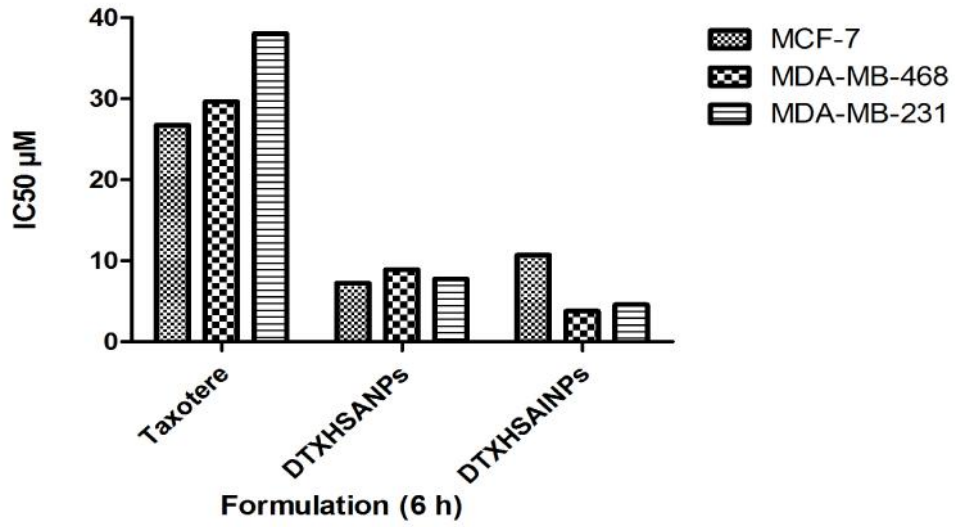

Figure 8. 8 Comparative IC_{50} Values of DTX formulations in MCF-7, MDA-MB-468 and MDA-MB-231 breast cancer cell lines (6 h).

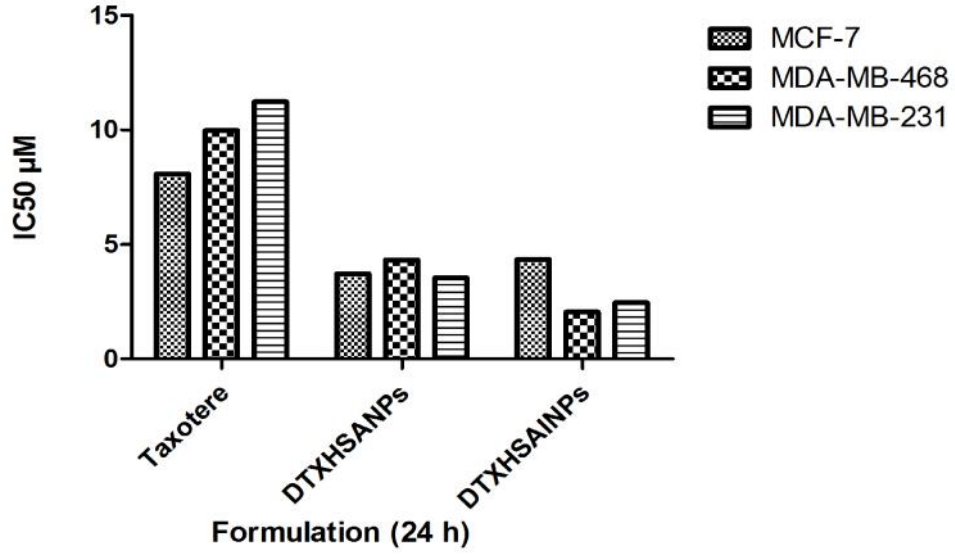

Figure 8. 9 Comparative IC_{50} Values of DTX formulations in MCF-7, MDA-MB-468 and MDA-MB-231 breast cancer cell lines (24 h).

% Cell viability and IC_{50} value were determined for Navelbine, VBT-HSA-NPs and VBT-HSA-INPs in MCF-7, MDA-MB-468 and MDA-MB-231 breast cancer cell lines and data presented in **Table 8.3 and Table 8.4.** Enhanced cytotoxic activity of VBT-HSA-INPs for MDA-MB-468 and MDA-MB-231 cells as compared to MCF-7 cells clearly demonstrates the high affinity of INPs towards EGFR positive cancer cells.

Table 8. 3 % Cell viability values of Navelbine, VBT-HSA-NPs and VBT-HSA-INPs in MCF-7, MDA-MB-468 and MDA-MB-231 breast cancer cell lines.

Formulation Concentration (15 µM/ ml)	% Cell viability* (After 24 h)			% Cell viability* (After 60 h)		
	MCF-7	MDA-MB-468	MDA-MB-231	MCF-7	MDA-MB-468	MDA-MB-231
Navelbine	49.21± 0.34	47.32± 0.59	45.46± 0.47	22.32± 0.21	26.41± 0.45	35.86± 0.82
VBT-HSA-NPs	29.31± 0.67	34.42± 0.79	32.49± 0.73	9.33± 0.96	14.34± 0.74	17.29± 0.34
VBT-HSA-INPs	34.12± 0.67	19.19± 0.47	25.63± 0.67	12.12± 0.67	7.98± 0.54	9.76± 0.45

* The experiment was performed in triplicate (n=3)

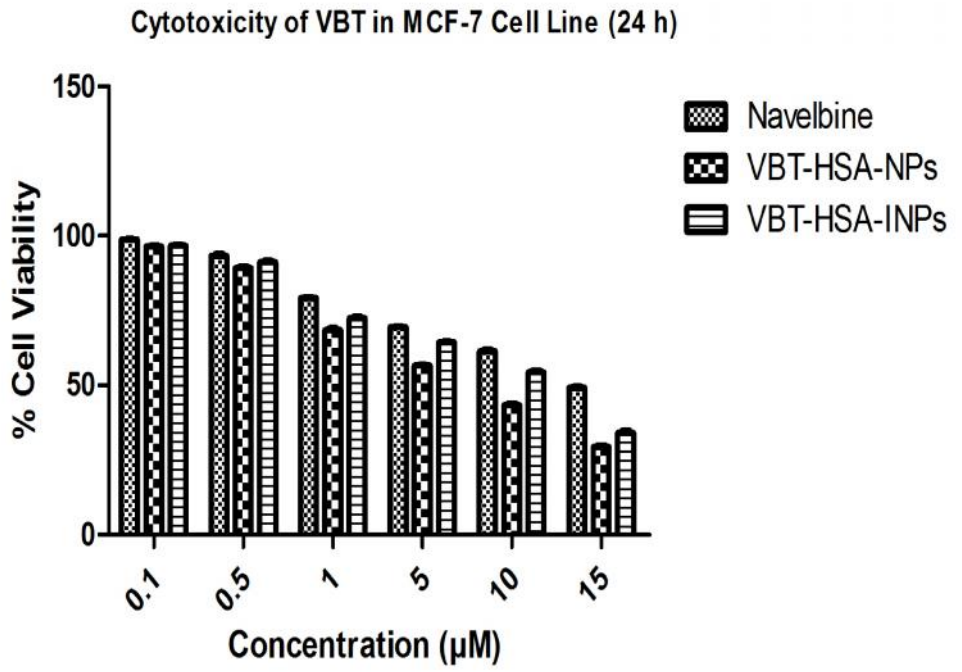

Figure 8. 10 Cytotoxicity of Different Formulations of VBT in MCF-7 Cell-line.

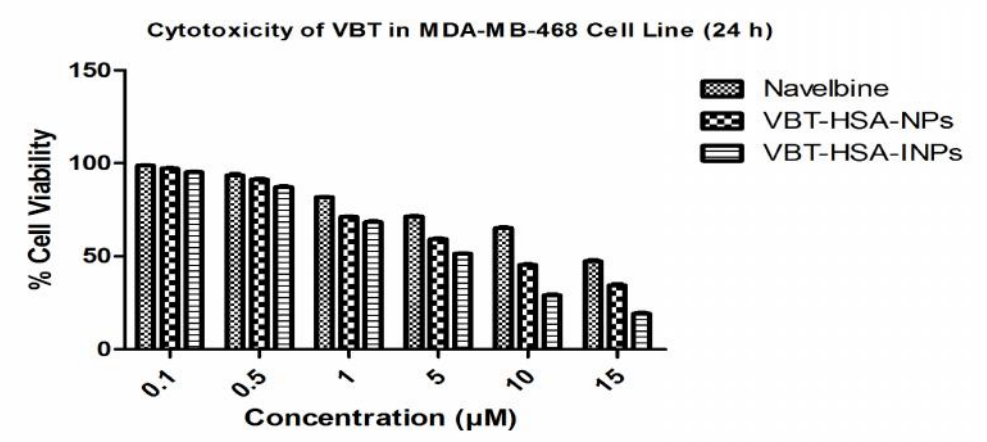

Figure 8. 11 Cytotoxicity of Different Formulations of VBT in MDA-MB-468 Cell-line.

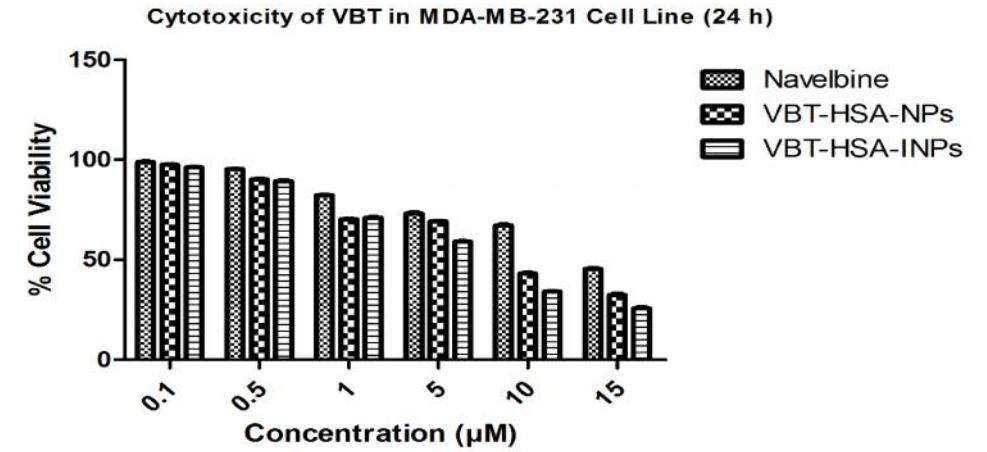

Figure 8. 12 Cytotoxicity of Different Formulations of VBT in MDA-MB-231 Cell-line.

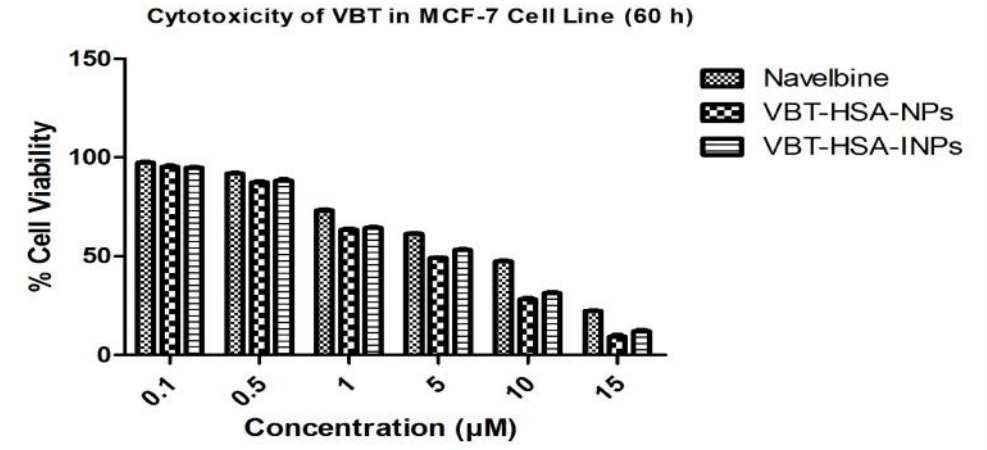

Figure 8. 13 Cytotoxicity of Different Formulations of VBT in MCF-7 Cell-line.

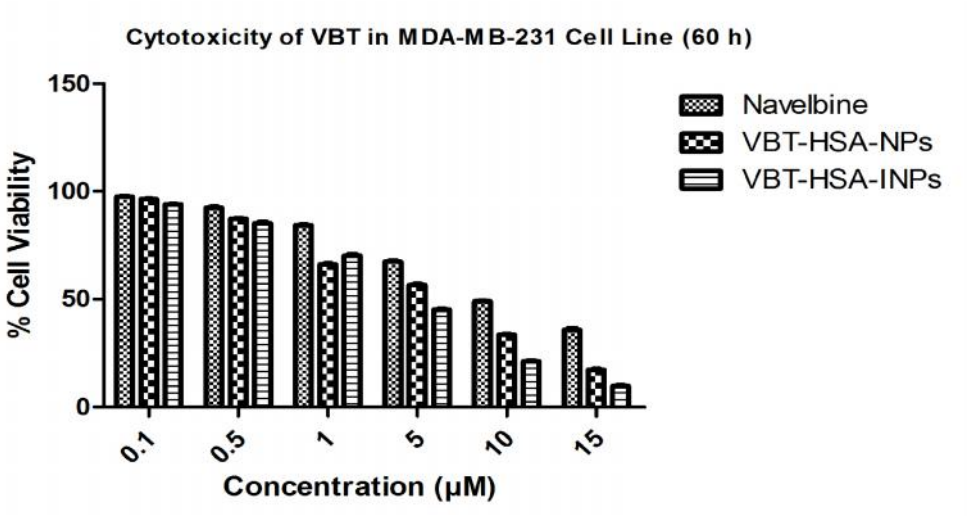

Figure 8. 14 Cytotoxicity of Different Formulations of VBT in MDA-MB-468 Cell-line.

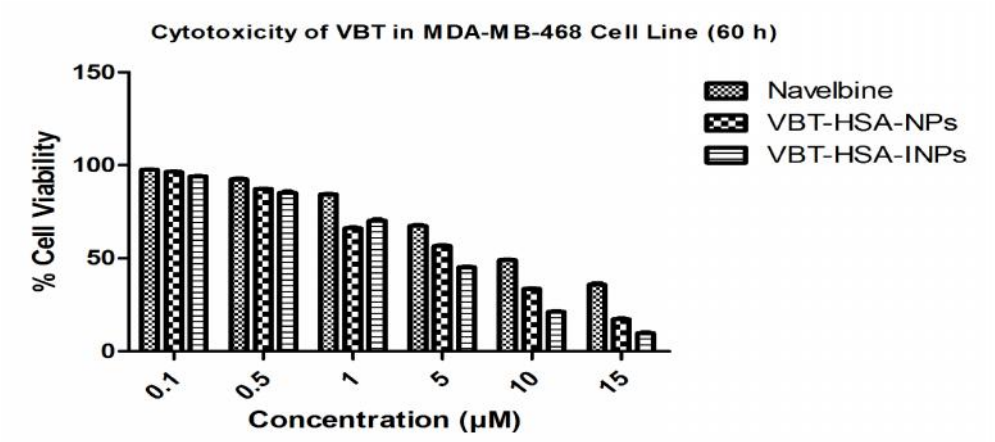

Figure 8. 15 Cytotoxicity of Different Formulations of VBT in MDA-MB-231 Cell-line.

Table 8. 4 IC_{50} values of Navelbine, VBT-HSA-NPs and VBT-HSA-INPs in MCF-7, MDA-MB-468 and MDA-MB-231 breast cancer cell lines.

Formulation	**IC_{50} Value (µM) (After 24 h)**			**IC_{50} Value (µM) (After 60 h)**		
	MCF-7	**MDA-MB-468**	**MDA-MB-231**	**MCF-7**	**MDA-MB-468**	**MDA-MB-231**
Navelbine	14.242	13.723	13.670	7.166	7.073	9.325
VBT-HSA-NPs	6.532	7.723	7.712	3.431	3.941	4.571
VBT-HSA-INPs	8.801	3.962	5.284	4.032	2.374	2.566

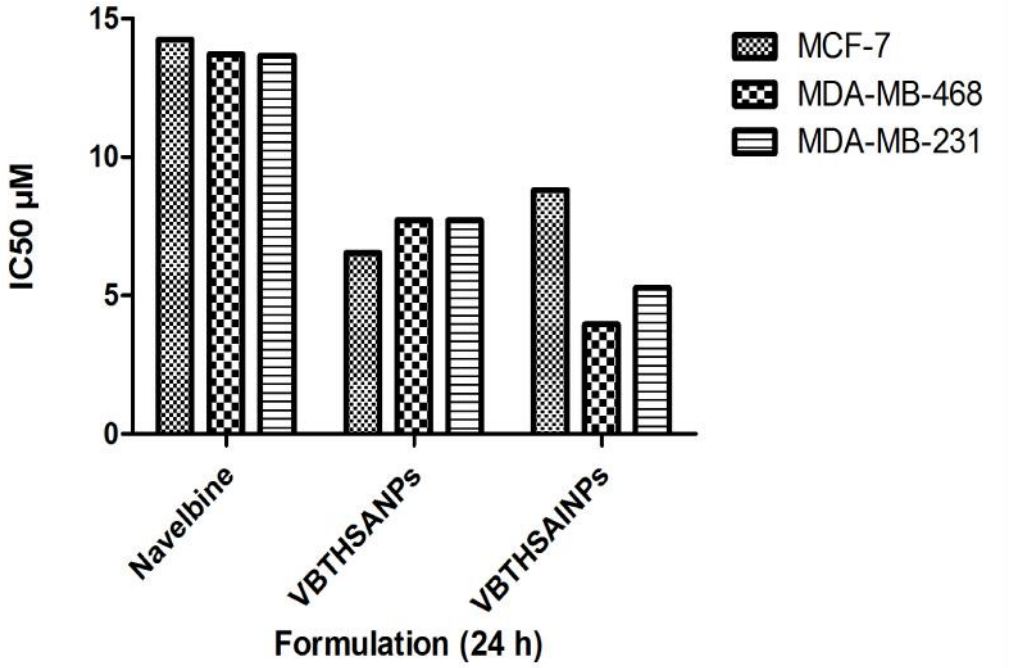

Figure 8. 16 Comparative IC_{50} Values of VBT formulations in MCF-7, MDA-MB-468 and MDA-MB-231 breast cancer cell lines (24 h).

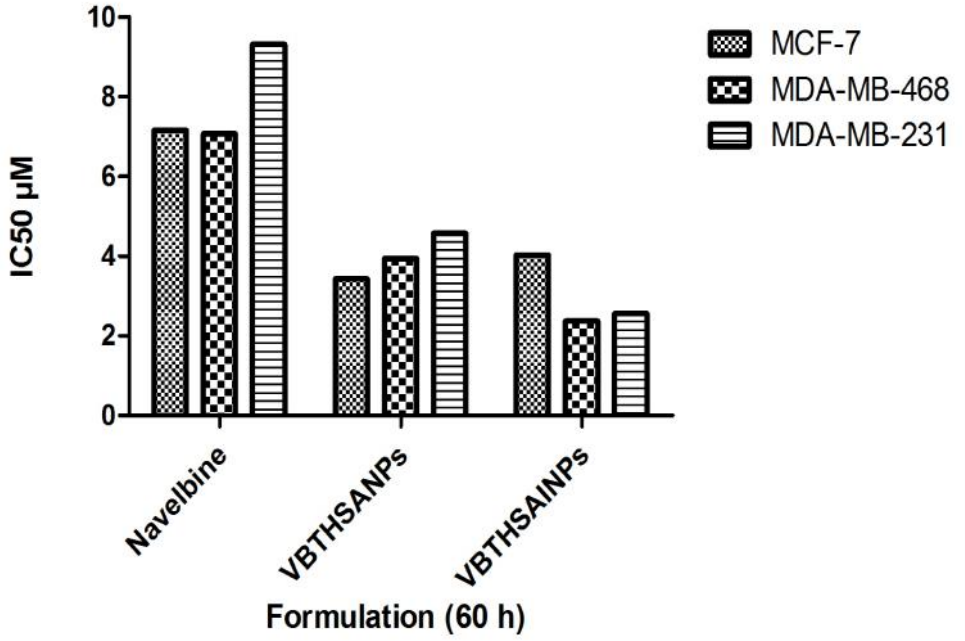

Figure 8. 17 Comparative IC_{50} Values of VBT formulations in MCF-7, MDA-MB-468 and MDA-MB-231 breast cancer cell lines (60 h).

8.4.2 Cellular Uptake

8.4.2.1 Qualitative cellular uptake by confocal microscopy

Qualitative uptake study results of coumarin, coumarin HSA-NPs and coumarin HSA-INPs (for DTX) by confocal microscopy in MDA-MB-468 and MDA-MB-231cell lines were represented in **Figure 8.18** and **Figure 8.19** respectively. The qualitative uptake study results of rhodamine, rhodamine HSA-NPs and rhodamine HSA-INPs (for VBT) by confocal microscopy in MDA-MB-468 and MDA-MB-231 cell lines were represented in **Figure 8.20** and **Figure 8.21** respectively. Our result confirmed that NPs showed augmented fluorescence activity in MDA-MB-468 and MDA-MB-231 cells treated with coumarin and rhodamine loaded INPs as compared to MCF-7 cells and results were represented in **Figure 8.22** and **Figure 8.23** respectively. The enhanced cellular uptake INPs in MDA-MB-468 cell lines explained on the basis of EGFR expression in cells and specificity of EGFR receptor mediated binding of INPs. Moreover, the enhanced uptake level of INPs can be attributed to the lesser binding and uptake of INPs by non-EGFR expressing MCF-7 cell lines.

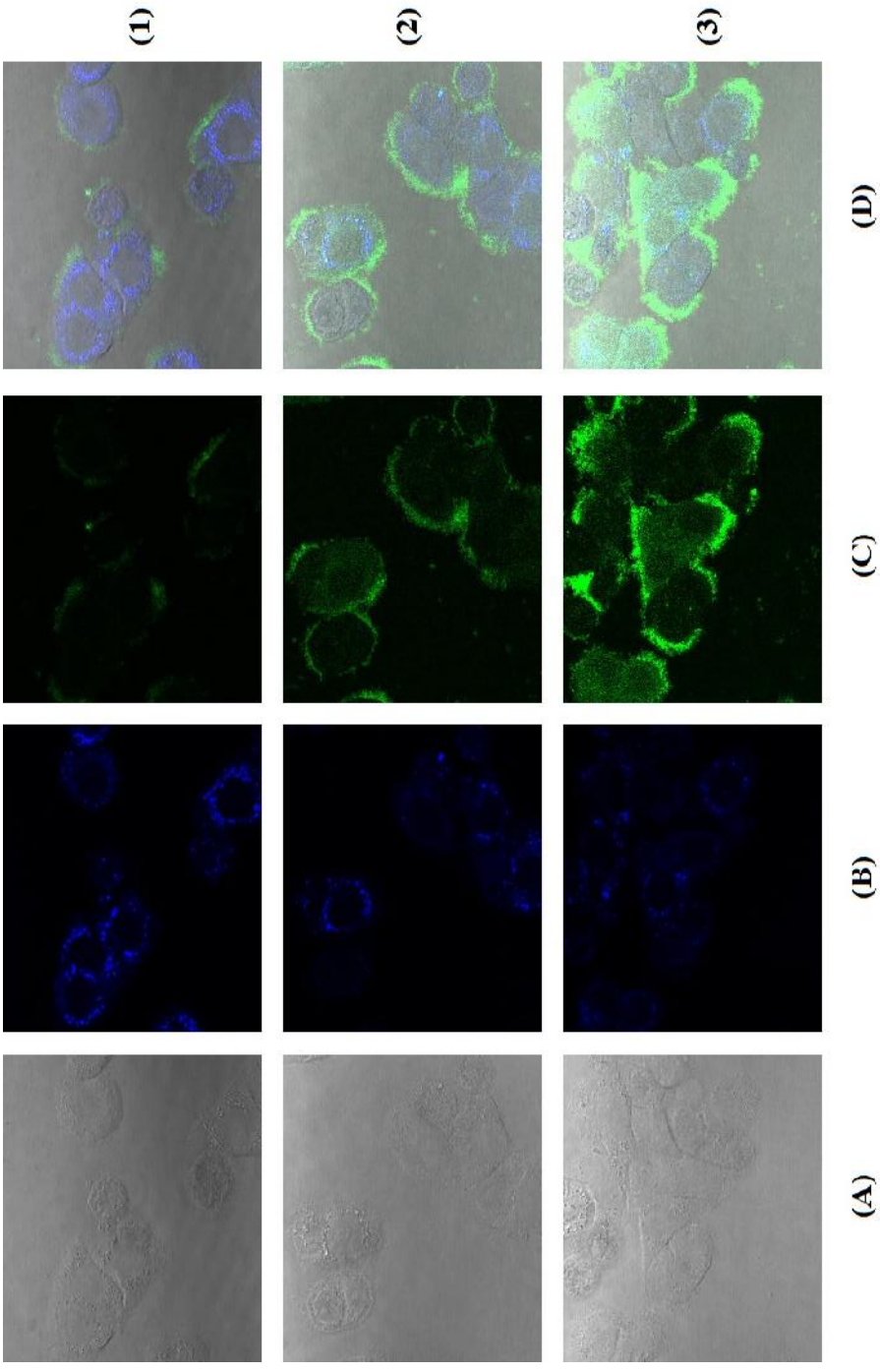

Figure 8. 18 Qualitative uptake of coumarin loaded formulations by confocal microscopy in MDA-MB-468 cell lines. 1=Coumarin 2=Coumarin-HSA-NPs, 3= Coumarin-HSA-INPs; A= Bright field, B=DAPI, C=Formulation Treated, D=Merged

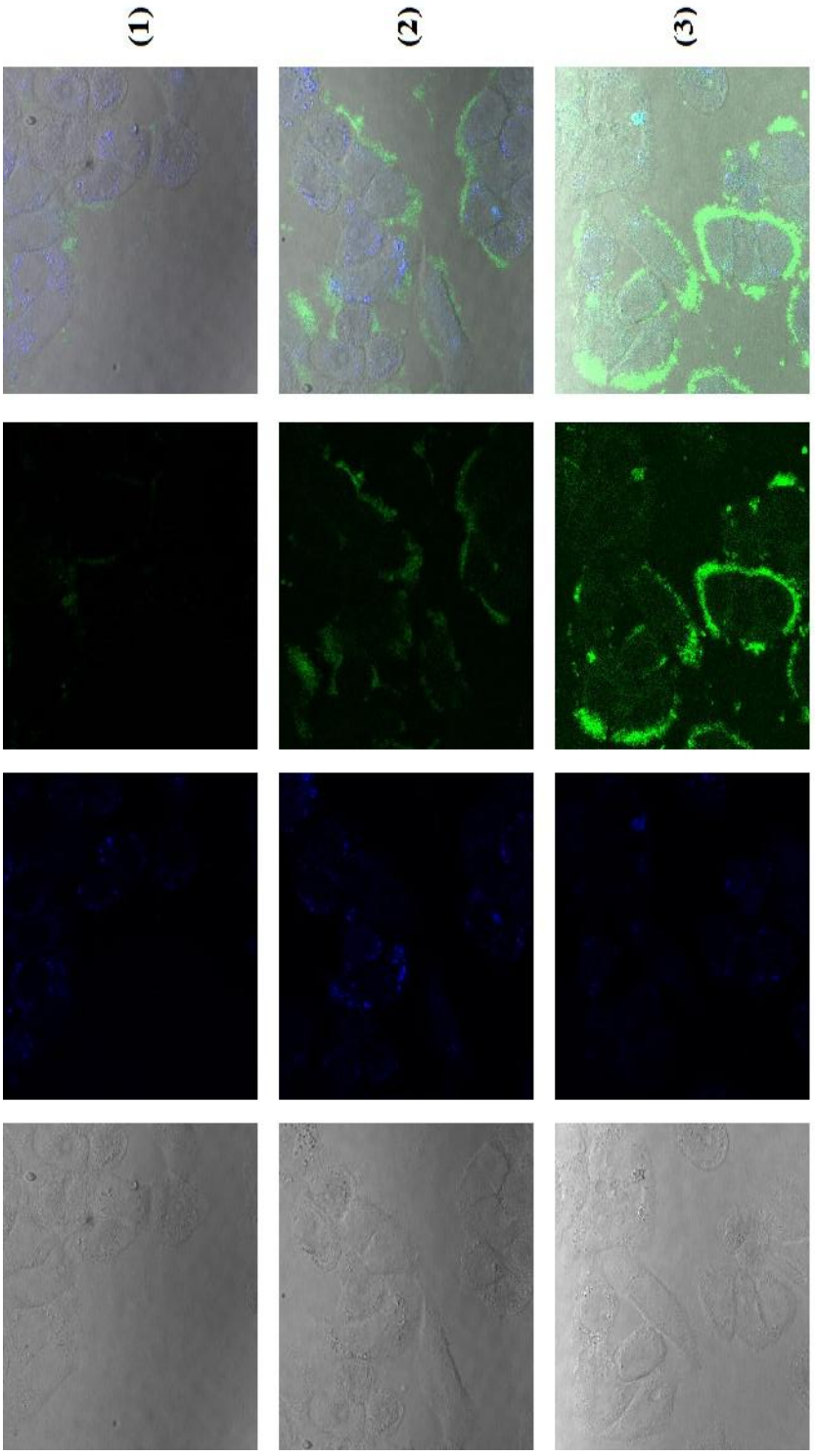

Figure 8. 19 Qualitative uptake of coumarin loaded formulations by confocal microscopy in MDA-MB-231 cell lines. 1=Coumarin 2=Coumarin-HSA-NPs, 3= Coumarin-HSA-INPs; A= Bright field, B=DAPI, C=Formulation Treated, D=Merged

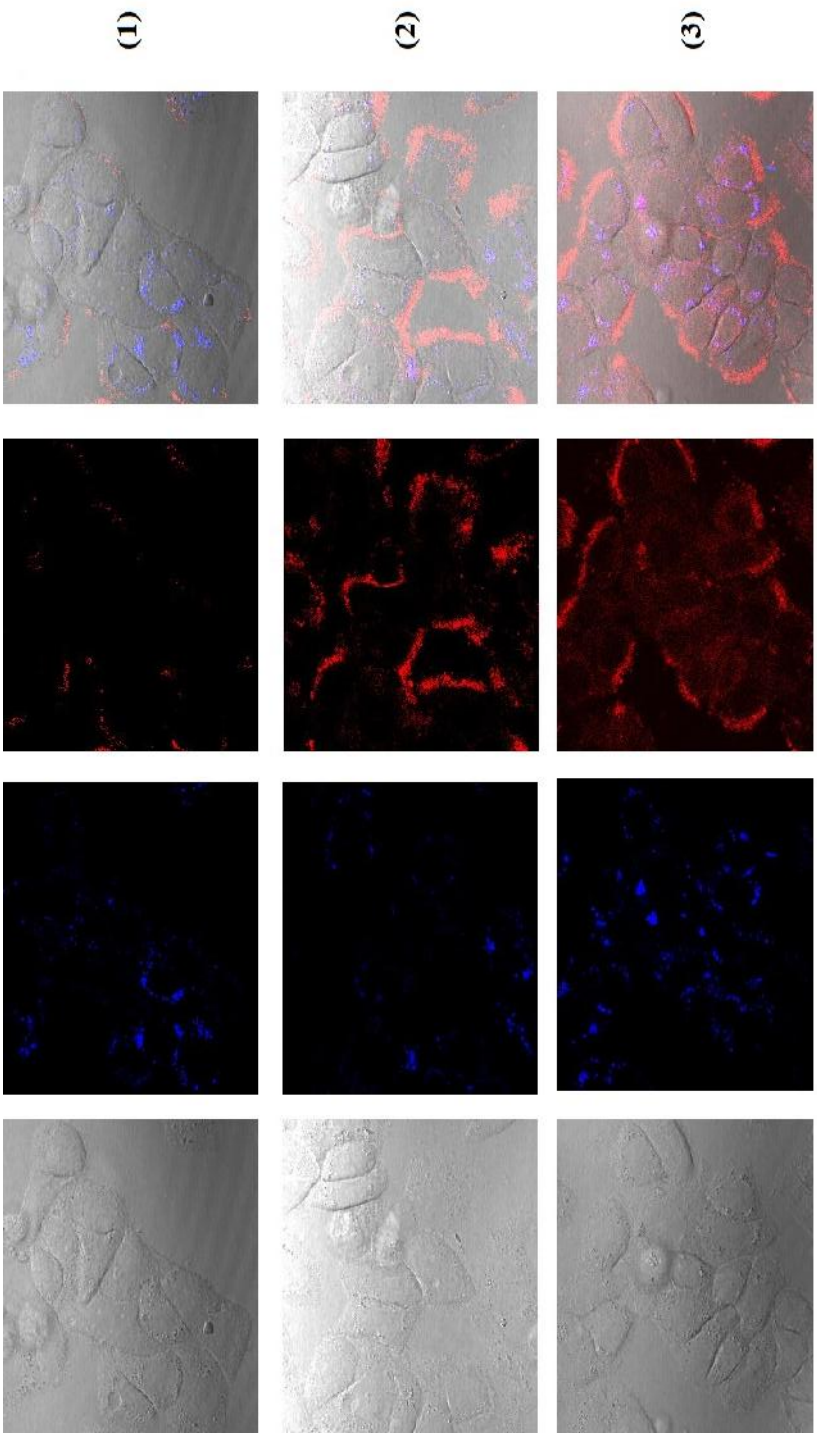

Figure 8. 20 Qualitative uptake of rhodamine loaded formulations by confocal microscopy in MDA-MB-468 cell lines. 1= Rhodamine 2= Rhodamine -HSA-NPs, 3= Rhodamine-HSA-INPs; A= Bright field, B=DAPI, C=Formulation Treated, D=Merged

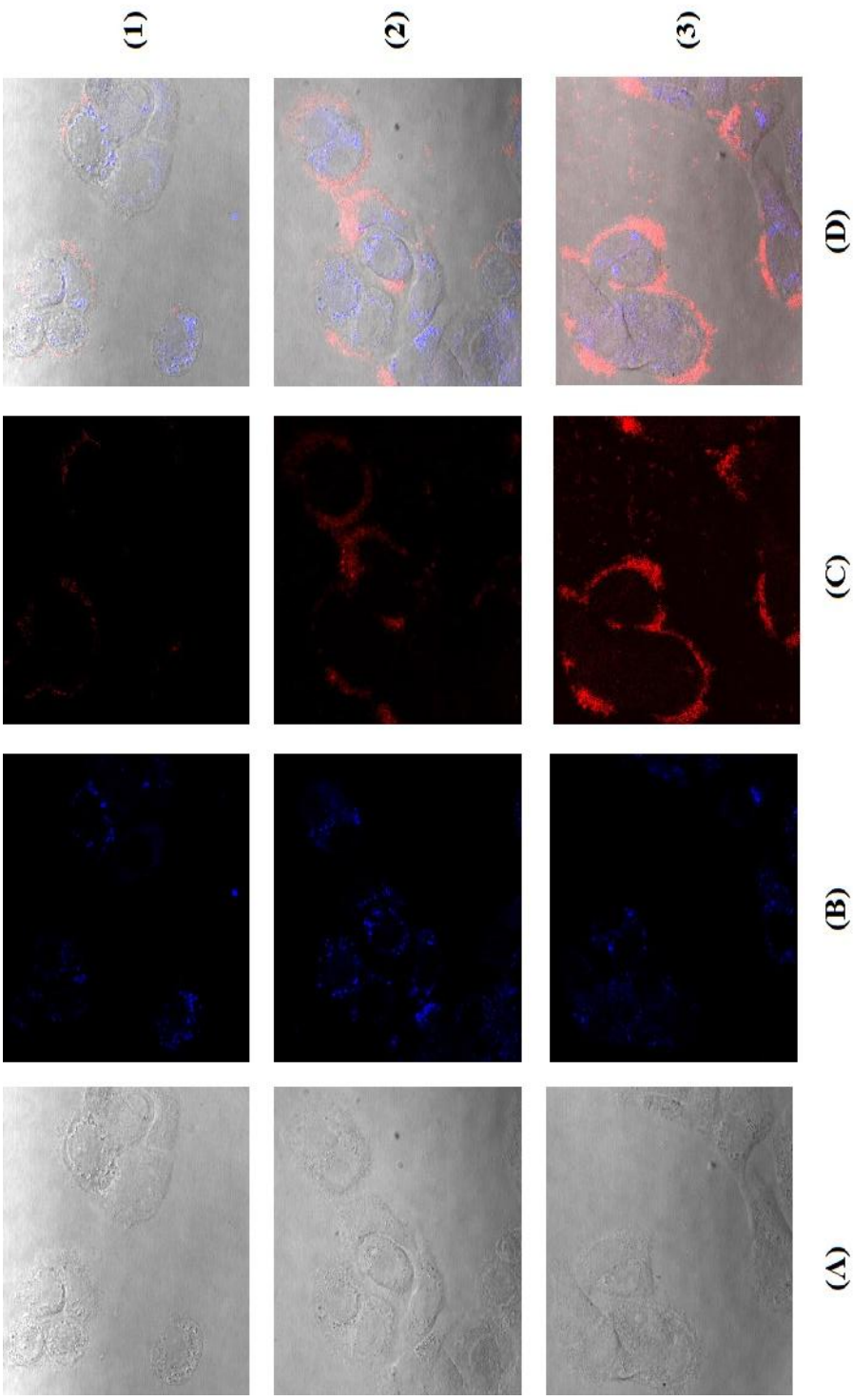

Figure 8. 21 Qualitative uptake of rhodamine loaded formulations by confocal microscopy in MDA-MB-231 cell lines. 1= Rhodamine 2= Rhodamine -HSA-NPs, 3= Rhodamine-HSA-INPs; A= Bright field, B=DAPI, C=Formulation Treated, D=Merged

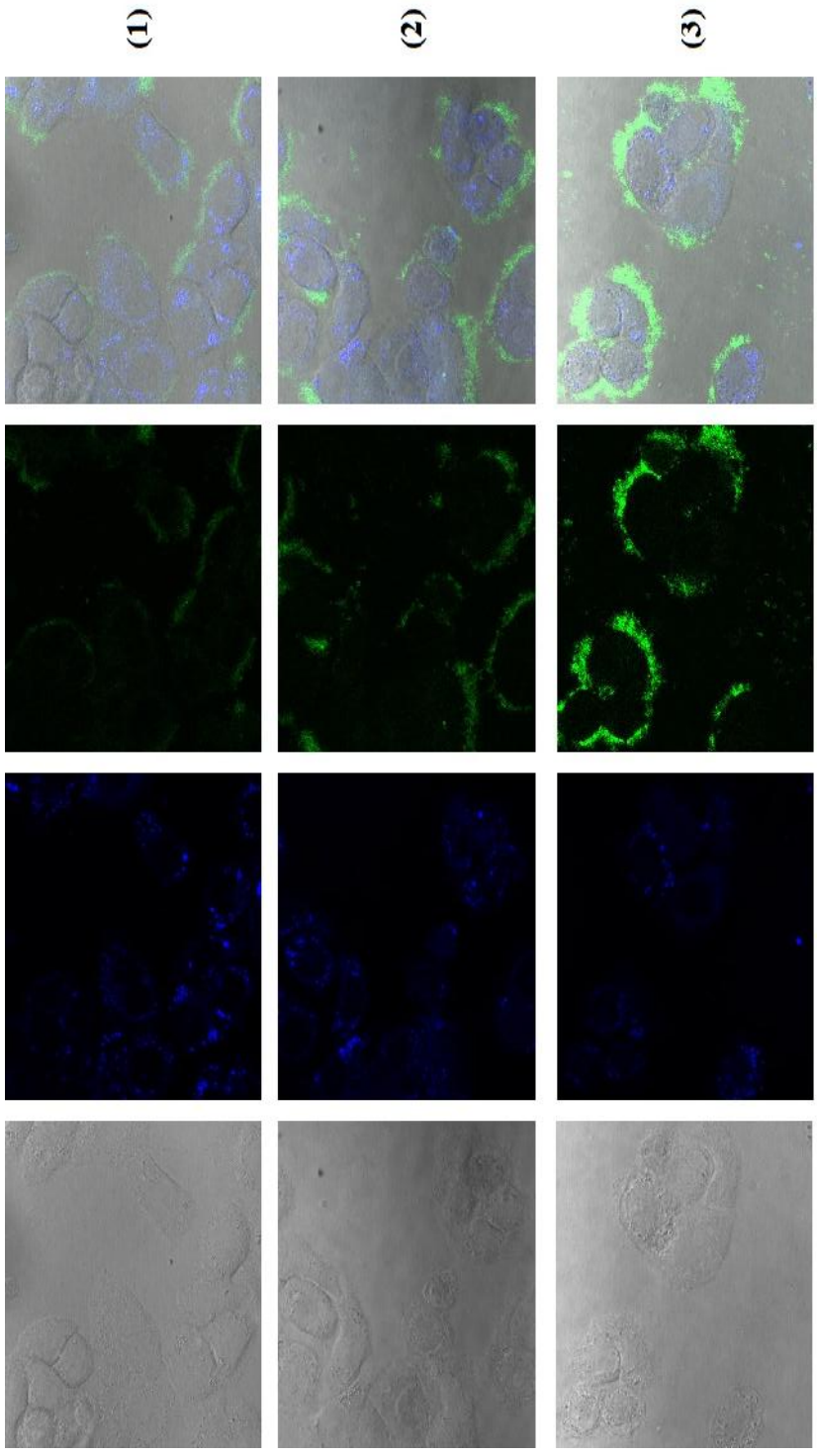

Figure 8. 22 Qualitative uptake of coumarin- HSA-INPs by confocal microscopy in MCF-7, MDA-MB-231 and MDA-MB-468 cell lines. 1= MCF-7, 2= MDA-MB-231, 3= MDA-MB-468; A= Bright field, B=DAPI, C= Coumarin- HSA-INPs Treated, D=Merged

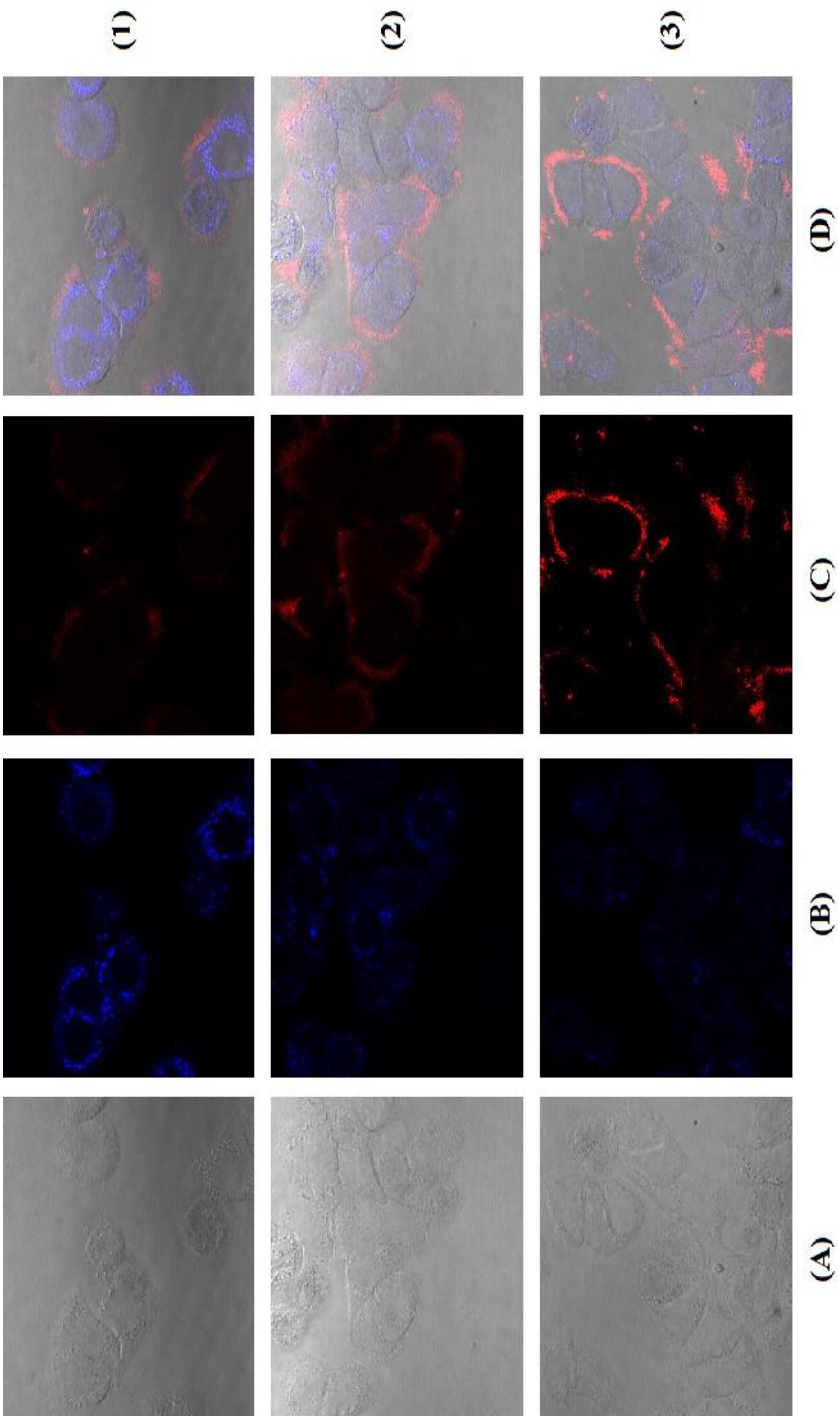

Figure 8. 23 Qualitative uptake of rhodamine- HSA-INPs by confocal microscopy in MCF-7, MDA-MB-231 and MDA-MB-468 cell lines. 1= MCF-7, 2= MDA-MB-231, 3= MDA-MB-468; A= Bright field, B=DAPI, C= Rhodamine- HSA-INPs Treated, D=Merged

8.4.2.2 Quantitative cellular uptake by FACS

Fluorescent property of 6-Coumarin and Rhodamine B was used for quantitative intracellular uptake of NPs in MDA-MB-468 cell line by FACS. The relative intracellular uptake of coumarin control, coumarin HSA-NPs and coumarin HSA-INPs was calculated using mean fluorescent index and is shown in **Figure 8.24** and **Figure 8.25**. As evident from **Figure 8.25** and data given in **Table 8.5** the MFI of coumarin HSA-INPs (1142.5 ± 19.3) is more than thrice than that of coumarin control (380.9 ± 21.1) and twice than that of coumarin HSA-NPs (575.8± 24.7) after 180 min due to receptor (EGFR) mediated endocytosis. Intracellular uptake was found to increase with time for all formulations from 60 to 180 min.

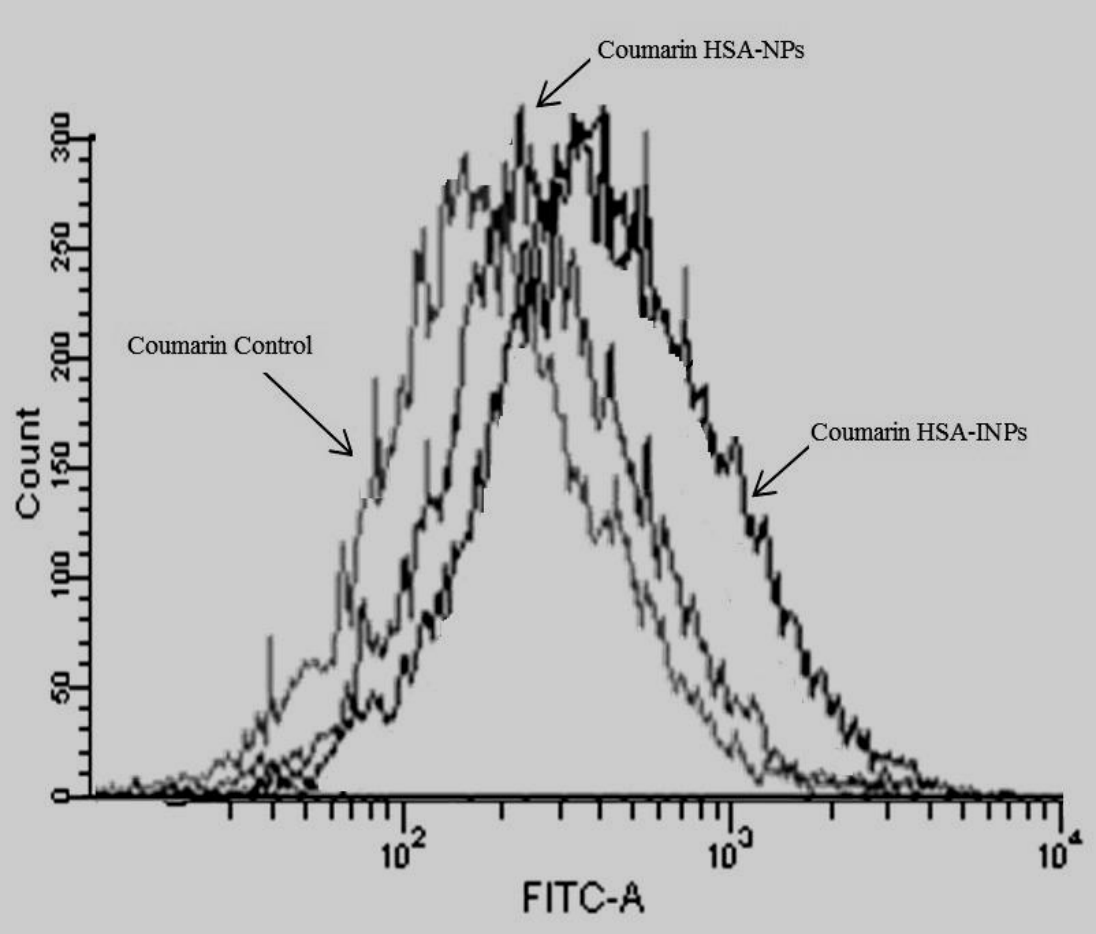

Figure 8. 24 Quantitative intracellular uptake of coumarin control, coumarin HSA-NPs and coumarin HSA-INPs in MDA-MB-468 cell line by FACS

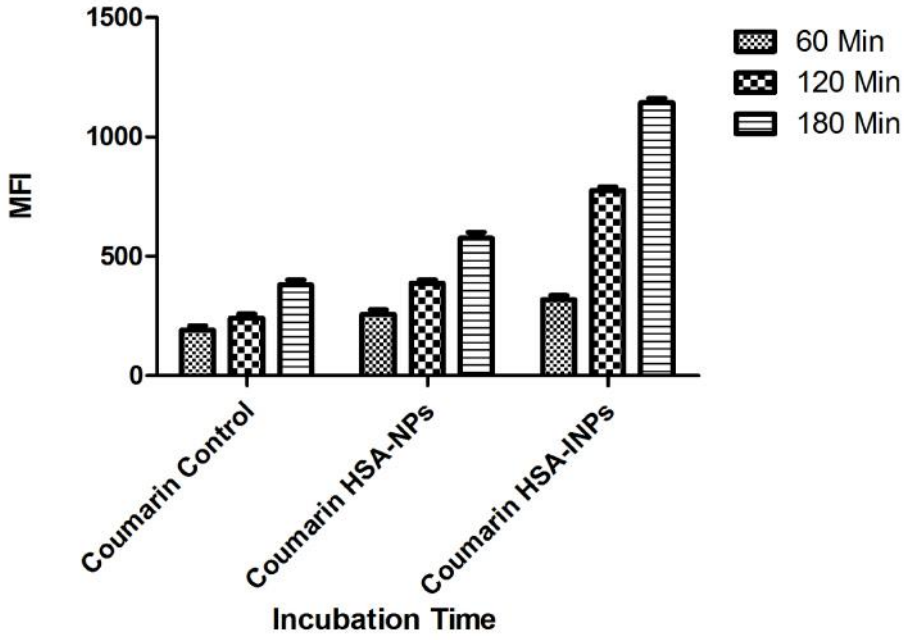

Figure 8. 25 Quantitative intracellular uptake (MFI) comparison of coumarin control, coumarin HSA-NPs and coumarin HSA-INPs in MDA-MB-468 cell line by FACS at different incubation time points. Data represented as mean ± S.D. (n=3)

Table 8. 5 MFI of coumarin control, coumarin HSA-NPs and coumarin HSA-INPs in MDA-MB-468 cell line by FACS at different incubation time points.

Treatment	Mean Fluorescence Intensity (MFI)*		
	60 min	120 min	180 min
Coumarin Control	190.6± 19.2	240.6± 17.5	380.9± 21.1
Coumarin HSA-NPs	256.7± 18.7	386.8± 15.6	575.8± 24.7
Coumarin HSA-INPs	318.3± 17.2	775.7± 14.9	1142.5± 19.3

* The experiment was performed in triplicate (n=3)

The relative intracellular uptake of rhodamine control, rhodamine HSA-NPs and rhodamine HSA-INPs was calculated using mean fluorescent index and is shown in **Figure 8.26** and **Figure 8.27**. As evident from **Figure 8.27** and data given in **Table 8.6** the MFI of rhodamine HSA-INPs (1245.6± 17.8) is about thrice than that of rhodamine control (420.9± 20.7) and 2.5 times than that of rhodamine HSA-NPs (508.7± 23.6) after 180 min

due to receptor (EGFR) mediated endocytosis. Intracellular uptake was found to increase with time for all formulations from 60 to 180 min.

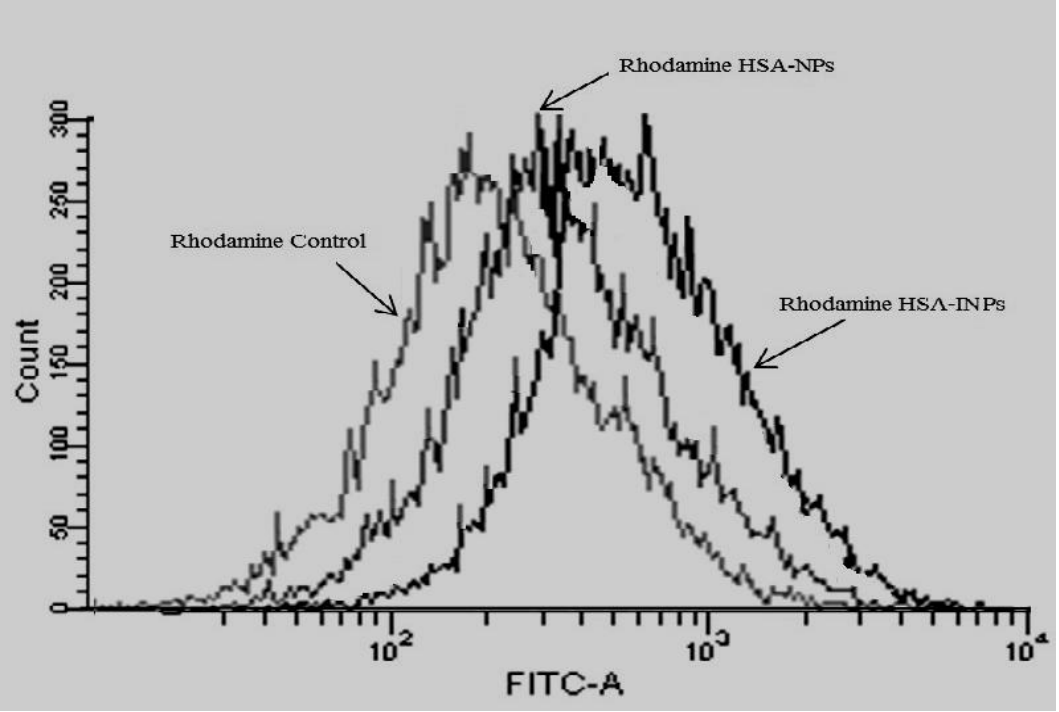

Figure 8. 26 Quantitative intracellular uptake of rhodamine control, rhodamine HSA-NPs and rhodamine HSA-INPs in MDA-MB-468 cell line by FACS

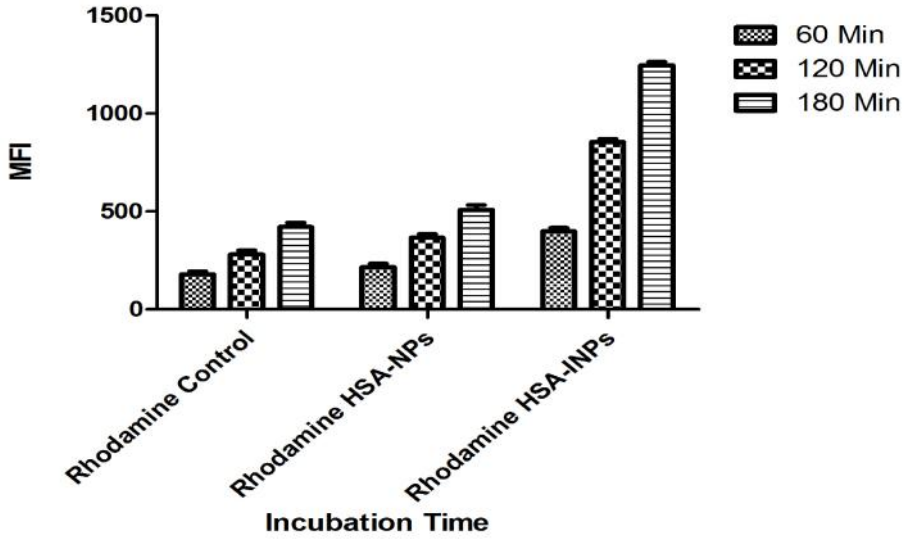

Figure 8. 27 Quantitative intracellular uptake (MFI) comparison of rhodamine control, rhodamine HSA-NPs and rhodamine HSA-INPs in MDA-MB-468 cell line by FACS at different incubation time points. Data represented as mean ± S.D. (n=3)

Table 8. 6 MFI of rhodamine control, rhodamine HSA-NPs and rhodamine HSA-INPs in MDA-MB-468 cell line by FACS at different incubation time points.

Treatment	Mean Fluorescence Intensity*		
	60 min	120 min	180 min
Rhodamine Control	178.8± 15.5	280.7± 19.3	420.9± 20.7
Rhodamine HSA-NPs	215.6± 17.6	365.7± 18.8	508.7± 23.6
Rhodamine HSA-INPs	398.7± 16.8	854.7± 14.4	1245.6± 17.8

* The experiment was performed in triplicate (n=3)

The intracellular uptake of NPs was incubation time dependent. The fluorescence intensity increased gradually with the incubation time and so also the uptake of NPs indicating time dependent uptake. Results clearly indicate the enhanced cellular uptake of INPs than non-conjugated and control system. The greater uptake of INPs can be explained on the basis of EGFR expression in cells and specificity of EGFR receptor mediated binding of INPs. Moreover, the enhanced uptake level of INPs can be attributed to the lesser exocytosis of the conjugated system than non-conjugated NPs. Together, all these contribute to the greater intracellular retention of INPs. Thus, higher cellular uptake observed with INPs is attributed to their greater intracellular delivery by receptor mediated endocytosis.

8.4.4 Apoptosis studies

Apoptosis studies were carried out using annexin V procedure to determine whether drug loaded NPs caused apoptosis or necrosis of MDA-MB-468 cells. The membrane phospholipid, phosphatidylserine is translocated from the inner cytoplasm of the plasma membrane to the outer cell surface soon after the induction of apoptosis, and annexin V protein has a strong, specific affinity for phosphatidylserine, while the membranes of dead and damaged cells are permeable to propidium iodide and allows identifying the late apoptotic cells and necrotic populations.

8.4.4.1 Docetaxel

The results showed significant fraction of necrotic, early and late apoptotic population of cells after exposure with Taxotere, DTX-HSA-NPs and DTX-HSA-INPs. Control group treated with PBS showed only 2.3% and 3.2 % cells in apoptotic phases after 24 and 48 h respectively. After 24 h and 48 hrs of exposure with Taxotere solution

only 6.2 and 5.4 % cells were in apoptotic phase (early and late apoptosis) whereas exposure with DTX-HSA-NPs and DTX-HSA-INPs showed 34.2 % and 60.9% cells in apoptotic phase which increased to 38.2% and 56.2%, respectively Shown in **Figure 8.28** and **Figure 8.29** respectively and data given in **Table 8.7**

Table 8. 7 Apoptosis studies in MDA-MB-468 cell line after treatment of (A1/B1) Control (PBS), (A2/B2) Taxotere (A3/B3) DTX-HSA-NPs and (A4/B4) DTX-HSA-INPs by FACS.

Drug (DTX)	24 h (A)				48 h (B)			
	Q1	Q2	Q3	Q4	Q1	Q2	Q3	Q4
Control	0.0	1.1	97.7	1.2	0.3	2.9	96.5	0.3
Taxotere	0.9	4.5	92.9	1.7	1.5	4.9	93.1	0.5
DTX-HSA-NPs	1.9	20.9	64.9	13.3	2.1	26.1	59.7	12.1
DTX-HSA-INPs	2.9	49.1	36.2	11.8	4.8	55.9	39.0	0.3

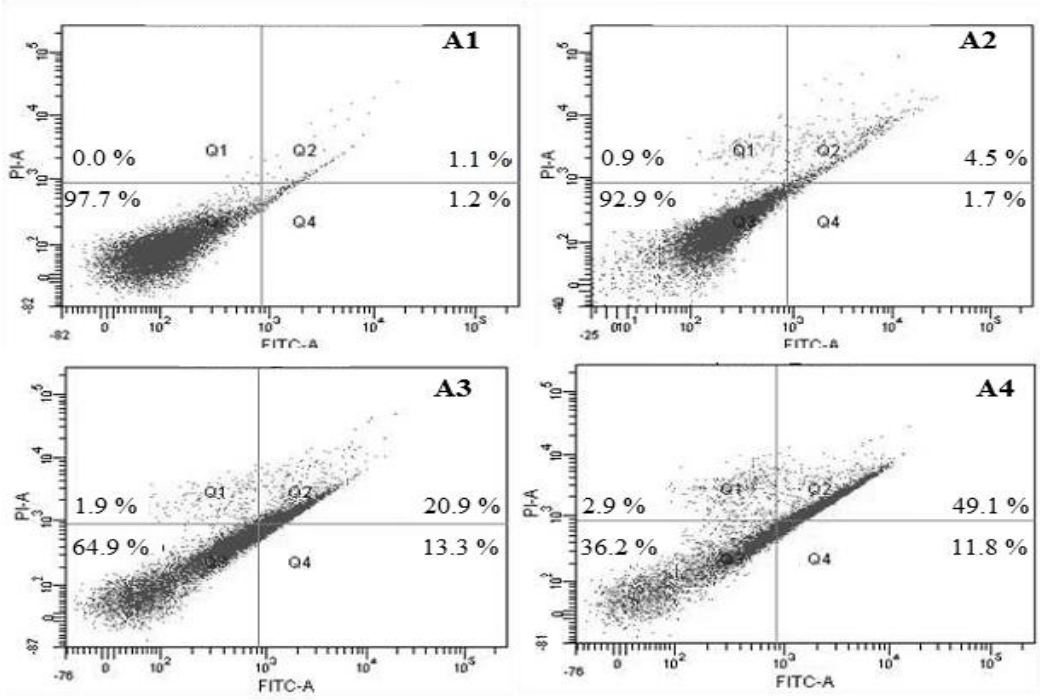

Figure 8. 28 Apoptosis estimation in MDA-MB-468 cell line
(A1) Control (PBS), (A2) Taxotere (A3) DTX-HSA-NPs and (A4) DTX-HSA-INPs; for (24h) by Annexin V-FITC and PI staining using FACS. Q1: Necrotic cells FITC (-) PI (+), Q:2 Late apoptosis FITC (+) PI (+), Q:3 Live FITC (-) PI(-), Q:4 Early apoptosis FITC (+) PI (-).

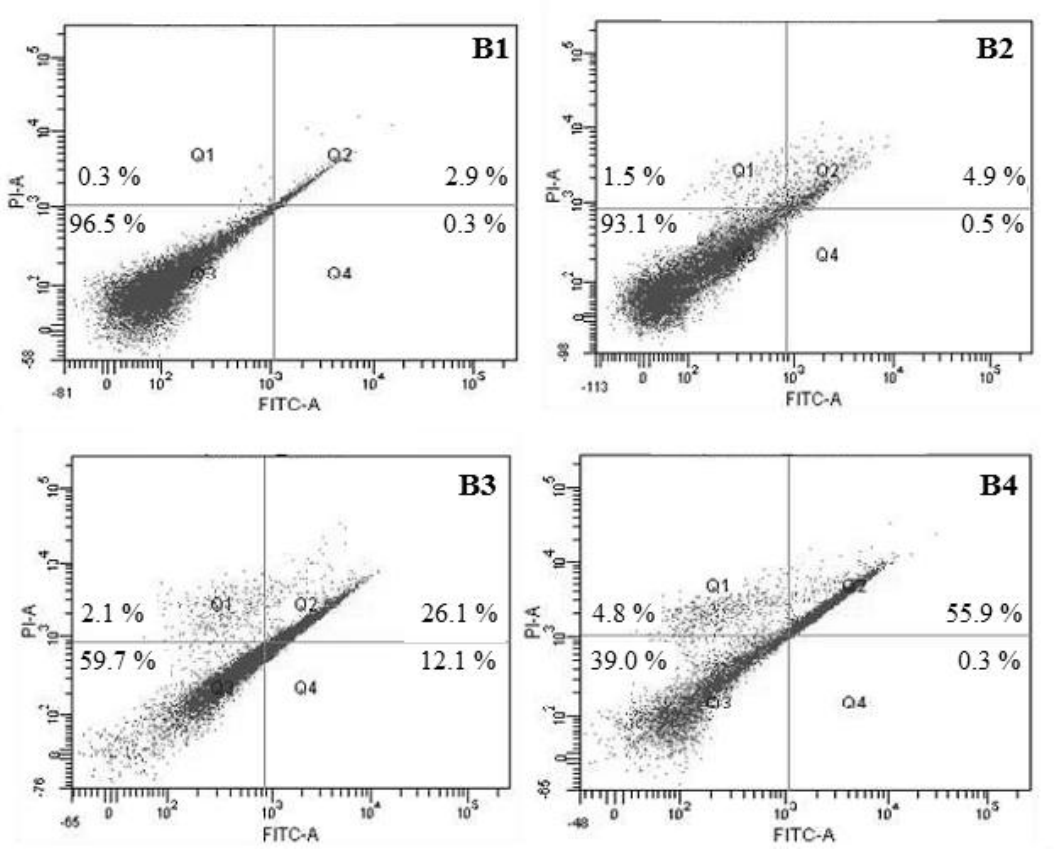

Figure 8. 29 Apoptosis estimation in MDA-MB-468 cell line
(B1) Control (PBS), (B2) Taxotere (B3) DTX-HSA-NPs and (B4) DTX-HSA-INPs; for (48 h) by Annexin V-FITC and PI staining using FACS. Q1: Necrotic cells FITC (-) PI (+), Q2: Late apoptosis FITC (+) PI (+), Q3: Live FITC (-) PI(-), Q:4 Early apoptosis FITC (+) PI (-).

With increase in exposure time from 24 h to 48 h the percentage of cells in early apoptotic phase decreased, at the same time percentage of cells in late apoptotic phase were found to be increased. This is possibly due to conversion of early apoptotic phase into late apoptotic phase. Similarly, percentage of cells undergone necrosis also increased with time but in less proportion than apoptosis indicating apoptosis as the possible mode of cell death. The augmented apoptotic activity of targeted INPs in comparison to Taxotere and non targeted NPs can be correlated with the results of quantitative uptake showing higher endocytosis. Apoptotic signals were possibly activated by targeted INPs at very low concentration than Taxotere and non targeted NPs. Targeted drug delivery showed enhanced apoptosis due to receptor mediated endocytosis which resulted in higher concentration of drug available for action at target site. Sustained cytoplasmic delivery of DTX from NPs coupled with scFv-EGFR antibody resulted in more enhanced therapeutic

potency of the NPs by apoptosis than Taxotere and non targeted NPs. Thus, INPs were able to cause significant increase in programmed cell death when compared with Taxotere and non targeted NPs nanoparticulate preparations, thus supporting the hypothesis that EGFR antibody conjugated INPs can serve as an effective delivery system for breast tumor targeting.

8.4.4.2 Vinorelbine

The results showed significant fraction of necrotic, early and late apoptotic population of cells after exposure with Navelbine, VBT-HSA-NPs and VBT-HSA-INPs. Control group treated with PBS showed only 2.1% and 4.0% cells in apoptotic phases. After 60 and 90 hrs of exposure Navelbine, VBT-HSA-NPs and VBT-HSA-INPs showed 5.9 %, 9.2 % and 24.5 % cells in apoptotic phase which increased to 6.4 %, 19.1 % and 54.7 %, respectively in **Figure 8.30** and **Figure 8.31** and data given in **Table 8.8.**

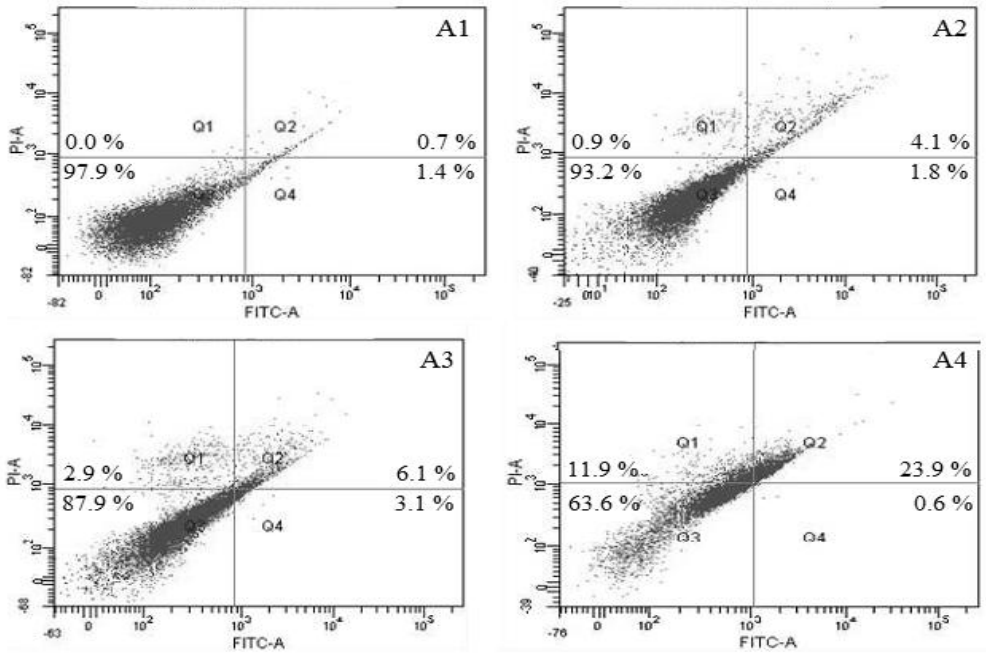

Figure 8. 30 Apoptosis estimation in MDA-MB-468 cell line

(A1) Control (PBS), (A2) Navelbine (A3) VBT-HSA-NPs and (A4) VBT-HSA-INPs; for (60h) by Annexin V-FITC and PI staining using FACS. Q1: Necrotic cells FITC (-) PI (+), Q2: Late apoptosis FITC (+) PI (+), Q3: Live FITC (-) PI(-), Q:4 Early apoptosis FITC (+) PI (-).

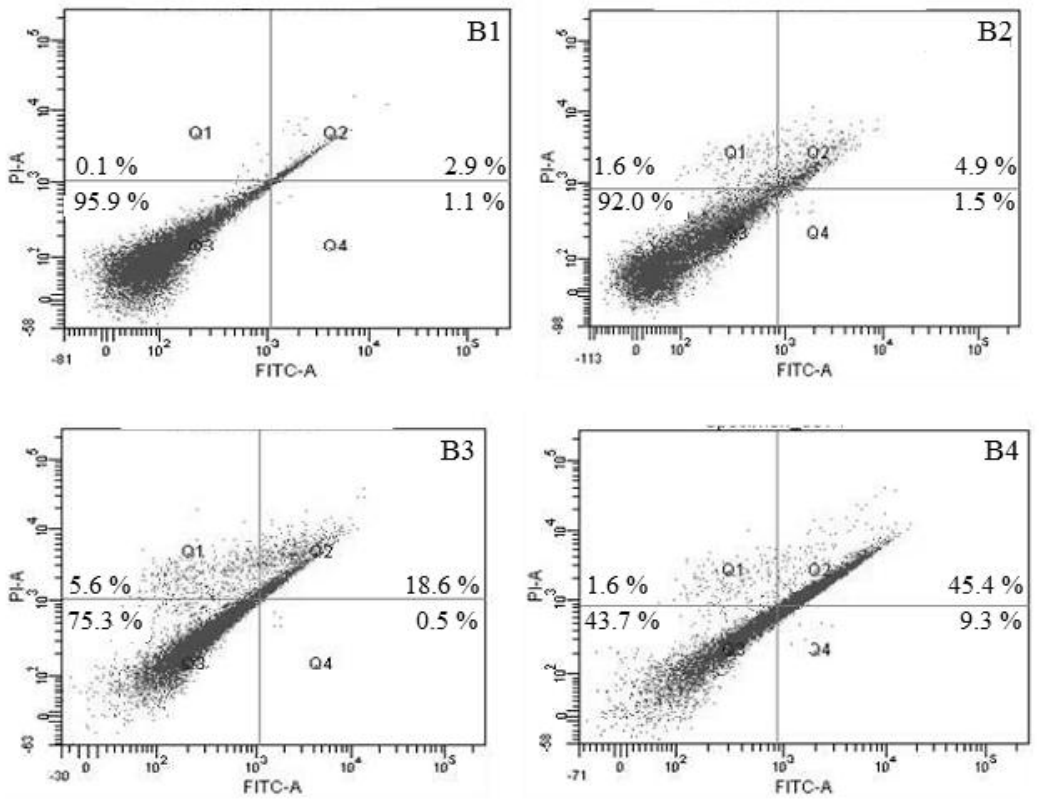

Figure 8. 31 Apoptosis estimation in MDA-MB-468 cell line
(B1) Control (PBS), (B2) Navelbine (B3) VBT-HSA-NPs and (B4) VBT-HSA-INPs; for (90 h) by Annexin V-FITC and PI staining using FACS. Q1: Necrotic cells FITC (-) PI +), Q2: Late apoptosis FITC (+) PI (+), Q3: Live FITC (-) PI(-), Q:4 Early apoptosis FITC (+) PI (-).

Table 8. 8 Apoptosis studies in MDA-MB-468 cell line after treatment of (A1/B1) Control (PBS), (A2/B2) Navelbine (A3/B3) VBT-HSA-NPs and (A4/B4) VBT-HSA-INPs using FACS.

VBT	60 h (A)				90 h (B)			
	Q1	Q2	Q3	Q4	Q1	Q2	Q3	Q4
Control	0.0	0.7	97.9	1.4	0.1	2.9	95.9	1.1
Navelbine	0.9	4.1	93.2	1.8	1.6	4.9	92.0	1.5
VBT-HSA-NPs	2.9	6.1	87.9	3.1	5.6	18.6	75.3	0.5
VBT-HSA-INPs	11.9	23.9	63.6	0.6	1.6	45.4	43.7	9.3

With increase in exposure time from 60 h to 90 h the percentage of cells in early apoptotic phase decreased, at the same time percentage of cells in late apoptotic phase

were found to be increased. This is possibly due to conversion of early apoptotic phase into late apoptotic phase. Similarly, percentage of cells undergone necrosis also increased with time but in less proportion than apoptosis indicating apoptosis as the possible mode of cell death. . The augmented apoptotic activity of targeted INPs in comparison to Navelbine and non targeted conjugated NPs can be correlated with the results of quantitative uptake showing higher endocytosis. Apoptotic signals were possibly activated by targeted INPs at very low concentration than Navelbine and non targeted NPs. Targeted drug delivery showed enhanced apoptosis due to receptor mediated endocytosis which resulted in higher concentration of drug available for action at target site. Sustained cytoplasmic delivery of VBT from NPs coupled with scFv-EGFR antibody resulted in more enhanced therapeutic potency of the NPs by apoptosis than Navelbine and non targeted NPs. Thus, INPs were able to cause significant increase in programmed cell death when compared with Navelbine and non targeted NPs nanoparticulate preparations, thus supporting the hypothesis that EGFR antibody conjugated INPs can serve as an effective delivery system for breast tumor targeting.

8.4.5 Cell cycle analysis

Drugs are known to act by different pharmacological actions which includes their effect on genes controlling the cell cycle and induction of pro- and anti-apoptotic genes. Docetaxel is known to inhibit cell growth and proliferation primarily through apoptosis inducing mechanism and cell cycle arrest. Hence, we investigated whether the pharmacological action of docetaxel would affect the proliferation of breast cancer cells by studying the distribution of DNA in cell cycle. The DNA distribution in cell cycle was studied to investigate the effect of prepared formulations on growth of MDA-MB-468 cells.

8.4.5.1 Docetaxel

Results of cell cycle analysis demonstrated that DTX treated cells showed stronger arrest at G0/G1 phase as compared to nanoparticulate formulations. INPs showed lesser percentage of cells at G0/G1 phase (36.57%) as compared to 63.24 % and 55.57 % cells in PBS (control) and Taxotere treated cells. INPs showed stronger arrest at G2/M phase (27.64 %) which was almost 1.67 times higher than Taxotere due receptor specific targeting shown in **Figure 8.31** and data given **Table 8.9**

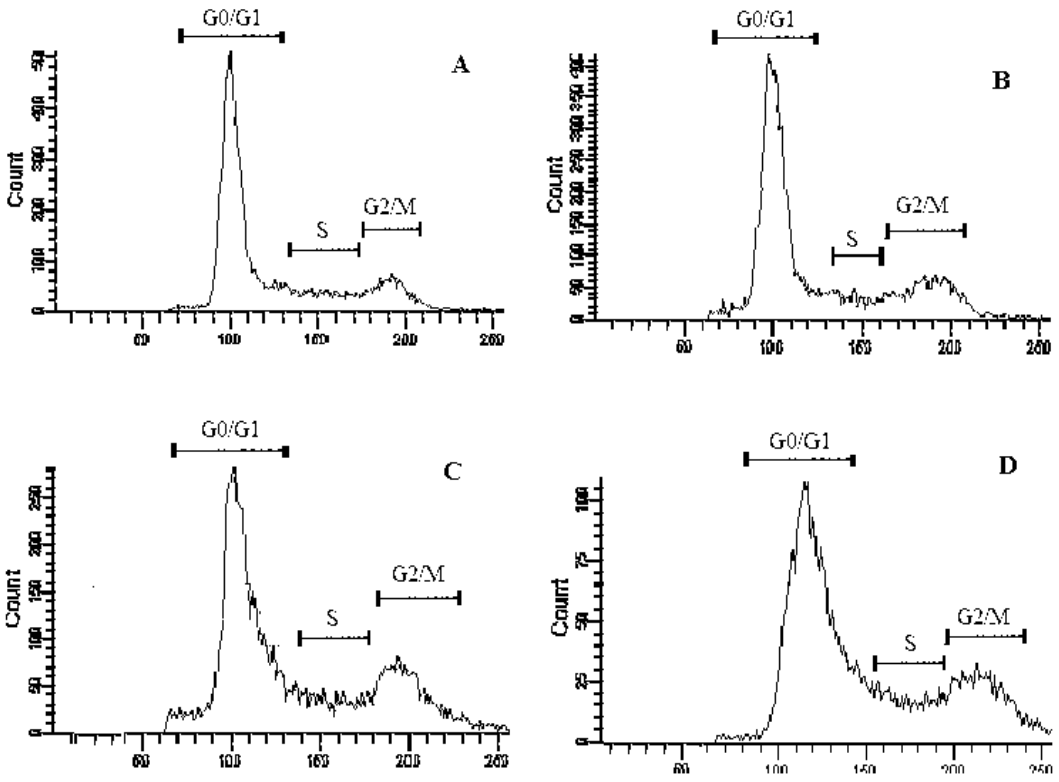

Figure 8. 32 Cell cycle analysis in MDA-MB-468 cell line after treatment of (a) Control (PBS), (b) Taxotere, (c) DTX-HSA-NPs and (d) DTX-HSA-INPs by PI staining using FACS

Table 8. 9 Cell cycle analysis in MDA-MB-468 cell line after treatment of (a) Control (PBS), (b) Taxotere, (c) DTX-HSA-NPs and (d) DTX-HSA-INPs by PI staining using FACS.

Treatment (24 h)	Phases		
	G0/G1	S	G2/M
Control (PBS)	63.24±1.25	26.22±0.82	10.54±0.61
Taxotere	55.57±2.45	28.28±6.65	**16.15±8.67**
DTX-HSA-NPs	45.86±3.31	32.80±3.66	21.34±3.25
DTX-HSA-INPs	36.57±4.74	35.79±6.12	**27.64±9.56**

8.4.5.2 Vinorelbine

Results of cell cycle analysis demonstrated that VBT treated cells showed stronger arrest at G0/G1 phase as compared to nanoparticulate formulations. INPs showed lesser

percentage of cells at G0/G1 phase (40.85%) as compared to 63. 34% and 58.74 % cells in PBS (control) and Navelbine treated cells. However, exposure to INPs showed stronger arrest at G2/M phase (24.31%) which was almost 2.05 times higher than Navelbine due receptor specific targeting shown in **Figure 8.32** and data given in **Table 8.10**

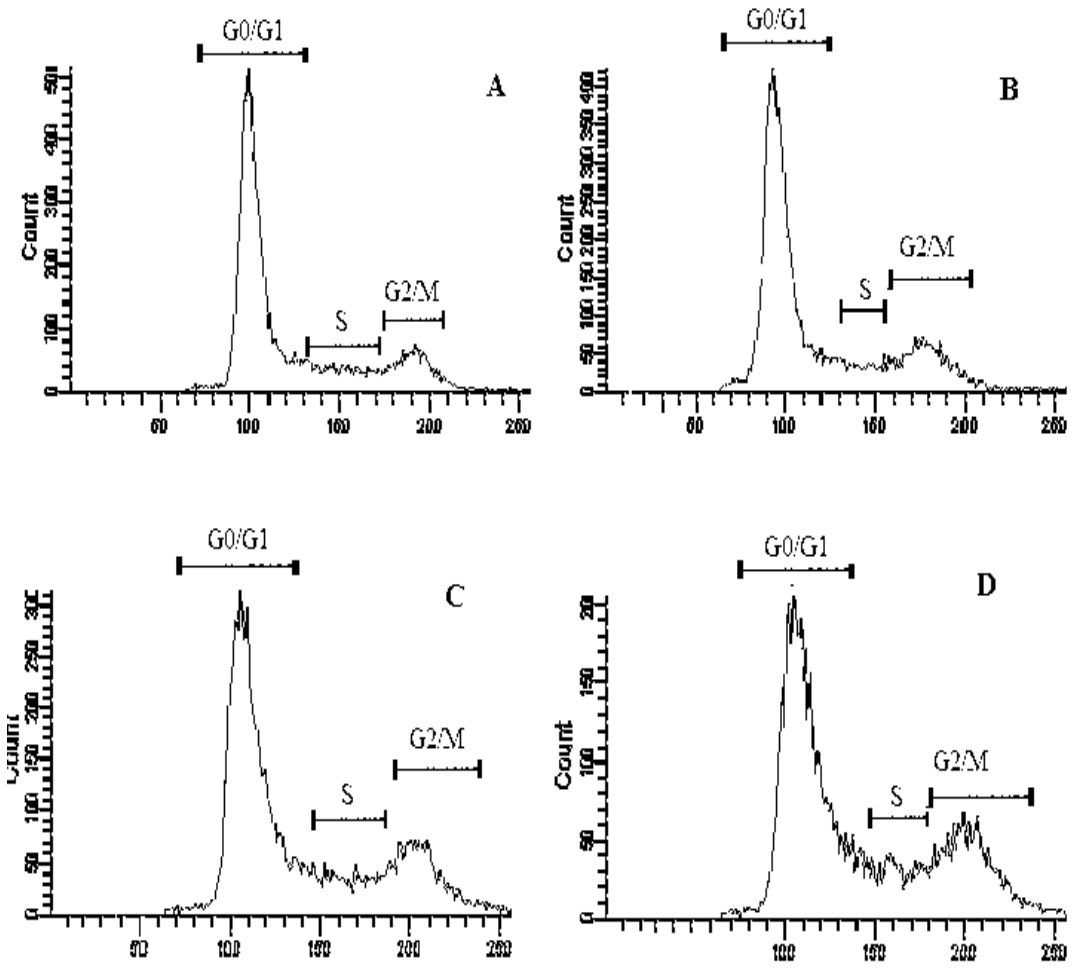

Figure 8. 33 Cell cycle analyses in MDA-MB-468 cell line after treatment of (a) Control (PBS), (b) Navelbine, (c) VBT-HSA-NPs and (d) VBT-HSA-INPs by PI staining using FACS.

Table 8. 10 Cell cycle analyses in MDA-MB-468 cell line after treatment of (a) Control (PBS), (b) Navelbine, (c) VBT-HSA-NPs and (d) VBT-HSA-INPs by PI staining using FACS.

Treatment (60 h)	**Phases**		
	G0/G1	S	G2/M
Control (PBS)	63.34±2.15	28.56±1.02	8.10±1.09
Navelbine	58.74±2.35	29.45±5.54	**11.81±6.51**
VBT-HSA-NPs	50.68±3.47	32.68±2.98	16.64±4.25
VBT-HSA-INPs	40.85±3.72	34.84±5.78	**24.31±10.63**

Greater efficiency of INPs in arresting more number of cells depends on the intracellular drug level in the target cells due to enhanced cellular uptake following receptor mediated endocytosis and sustained drug release as compared to drug solution and non- targeted NPs.

8.5 References:

1. Papouchado B, Erickson LA, Rohlinger AL, Hobday TJ, Erlichman C, Ames MM, et al. Epidermal growth factor receptor and activated epidermal growth factor receptor expression in gastrointestinal carcinoids and pancreatic endocrine carcinomas. Mod Pathol. 2005 Oct;18(10):1329-35.
2. Berridge MV, Herst PM, Tan AS. Tetrazolium dyes as tools in cell biology: new insights into their cellular reduction. Biotechnol Annu Rev. 2005;11:127-52.
3. Berridge MV, Tan AS. Characterization of the cellular reduction of 3-(4,5-dimethylthiazol-2-yl)-2,5-diphenyltetrazolium bromide (MTT): subcellular localization, substrate dependence, and involvement of mitochondrial electron transport in MTT reduction. Arch Biochem Biophys. 1993 Jun;303(2):474-82.
4. Castino R, Demoz M, Isidoro C. Destination 'lysosome': a target organelle for tumour cell killing? J Mol Recognit. 2003 Sep-Oct;16(5):337-48.
5. Sly WS, Vogler C. Brain-directed gene therapy for lysosomal storage disease: going well beyond the blood- brain barrier. Proc Natl Acad Sci U S A. 2002 Apr 30;99(9):5760-2.
6. Bareford LM, Swaan PW. Endocytic mechanisms for targeted drug delivery. Adv Drug Deliv Rev. 2007 Aug 10;59(8):748-58.
7. Wang T, Bai J, Jiang X, Nienhaus GU. Cellular uptake of nanoparticles by membrane penetration: a study combining confocal microscopy with FTIR spectroelectrochemistry. ACS Nano. 2012 Feb 28;6(2):1251-9.
8. Zhang LW, Monteiro-Riviere NA. Use of confocal microscopy for nanoparticle drug delivery through skin. J Biomed Opt. 2013 Jun;18(6):061214.
9. Ibuki Y, Toyooka T. Nanoparticle uptake measured by flow cytometry. Methods Mol Biol. 2012;926:157-66.
10. Kanzawa T, Kondo Y, Ito H, Kondo S, Germano I. Induction of autophagic cell death in malignant glioma cells by arsenic trioxide. Cancer Res. 2003 May 1;63(9):2103-8.
11. Salma J, McDermott JC. Suppression of a MEF2-KLF6 survival pathway by PKA signaling promotes apoptosis in embryonic hippocampal neurons. J Neurosci. 2012 Feb 22;32(8):2790-803.
12. Panyam J, Labhasetwar V. Biodegradable nanoparticles for drug and gene delivery to cells and tissue. Adv Drug Deliv Rev. 2003 Feb 24;55(3):329-47.